

1 **A mutation-independent approach via transcriptional upregulation of a disease**
2 **modifier gene rescues muscular dystrophy *in vivo***

3

4 Dwi U. Kemaladewi^{1,*}, Prabhpreet S. Bassi^{1,2,*}, Steven Erwood^{1,2}, Dhekra Al-Basha^{3,4},
5 Kinga I. Gawlik⁵, Kyle Lindsay¹, Ella Hyatt¹, Rebekah Kember¹, Kara M. Place¹, Ryan M.
6 Marks¹, Madeleine Durbeej⁵, Steven A. Prescott^{3,4,6}, Evgueni A. Ivakine^{1,**}, Ronald D.
7 Cohn^{1,2,7,**}

8

9 ¹Program in Genetics and Genome Biology, the Hospital for Sick Children Research
10 Institute, Toronto, Canada

11 ²Department of Molecular Genetics, University of Toronto, Canada

12 ³Program in Neuroscience and Mental Health, the Hospital for Sick Children Research
13 Institute, Toronto, Canada

14 ⁴Department of Physiology, University of Toronto, Canada

15 ⁵Unit of Muscle Biology, Department of Experimental Medical Science, Lund University,
16 Lund, Sweden

17 ⁶Institute of Biomaterials and Biomedical Engineering, University of Toronto, Canada

18 ⁷Department of Pediatrics, the Hospital for Sick Children, Toronto, Canada

19 *These authors contributed equally to this work

20 **These authors contributed equally to this work

21

22

23

24 **Introductory paragraph**

25 Identification of genetic modifiers has provided critically important insights into the
26 pathogenesis and heterogeneity of disease phenotypes in individuals affected by
27 neuromuscular disorders (NMDs). Targeting modifier genes to improve disease
28 phenotypes could be especially beneficial in cases where the causative genes are large,
29 structurally complex and the mutations are heterogeneous. Here, we report a mutation-
30 independent strategy to upregulate expression of a compensatory disease-modifying
31 gene in Congenital Muscular Dystrophy type 1A (MDC1A) using a CRISPR/dCas9-
32 based transcriptional activation system.

33 MDC1A is caused by nonfunctional Laminin $\alpha 2$, which compromises muscle fibers
34 stability and axon myelination in peripheral nerves ¹. Transgenic overexpression of
35 *Lama1*, encoding a structurally similar protein Laminin $\alpha 1$, ameliorates muscle wasting
36 and paralysis in the MDC1A mouse models, demonstrating its important role as a
37 disease modifier ². Yet, upregulation of *Lama1* as a postnatal gene therapy is hampered
38 by its large size, which exceeds the current genome packaging capacity of clinically
39 relevant delivery vehicles such as adeno-associated viral vectors (AAVs).

40 In this study, we use the CRISPR/dCas9-based transcriptional activation system to
41 upregulate *Lama1*. This system is comprised of catalytically inactive *S. aureus* Cas9
42 (dCas9) fused to VP64 transactivation domains and sgRNAs targeting the *Lama1*
43 promoter. We first demonstrate robust upregulation of *Lama1* in myoblasts, and
44 following AAV9-mediated intramuscular delivery, in skeletal muscles of *dy^{2j}/dy^{2j}* mouse
45 model of MDC1A.

46 We therefore assessed whether systemic upregulation of *Lama1* would yield therapeutic
47 benefits in *dy^{2j}/dy^{2j}* mice. When the intervention was started early in pre-symptomatic
48 *dy^{2j}/dy^{2j}* mice, *Lama1* upregulation prevented muscle fibrosis and hindlimb paralysis. An
49 important question for future therapeutic approaches for a variety of disorders relates to
50 the therapeutic window and phenotypic reversibility. This is particularly true for muscular
51 dystrophies as it has long been hypothesized that fibrotic changes in skeletal muscle
52 represent an irreversible disease state that would impair any therapeutic intervention at
53 advanced stages of the disease. Here, we demonstrate that dystrophic features and
54 disease progression were significantly improved and reversed when the treatment was
55 initiated in symptomatic 3-week old *dy^{2j}/dy^{2j}* mice with already-apparent hind limb
56 paralysis and significant muscle fibrosis.

57 Collectively, our data demonstrate the feasibility and therapeutic benefit of
58 CRISPR/dCas9-mediated modulation of a disease modifier gene, which opens up an
59 entirely new and mutation-independent treatment approach for all MDC1A patients.
60 Moreover, this treatment strategy provides evidence that muscle fibrosis can be
61 reversible to some degree, thus extending the therapeutic window for this disorder. Our
62 data provide a proof-of-concept strategy that can be applied to a variety of disease
63 modifier genes and a powerful therapeutic approach for various inherited and acquired
64 diseases.

65

66

67 Congenital muscular dystrophy 1A (MDC1A) is an autosomal recessive neuromuscular
68 disease associated with a high degree of morbidity and mortality in early childhood ¹. It is
69 caused by mutations in the *LAMA2* gene encoding Laminin α 2 chain (LAMA2), which
70 interacts with the β 1 and γ 1 chains to form the heterotrimer Laminin-211, an extracellular
71 matrix protein (reviewed in ³). Laminin-211 interacts with α -dystroglycan and α 7 β 1
72 integrin in skeletal muscle and Schwann cells, providing the necessary roles such as
73 survival and stability of myotubes, as well as proper neurite growth, axon myelination
74 and migration of Schwann cells. Lack of Laminin-211 in MDC1A causes degeneration of
75 skeletal muscle and impaired Schwann cell differentiation, resulting in a cascade of
76 secondary events including apoptosis/necrosis of muscle fibers, inflammation, and
77 fibrosis, which ultimately precipitate the disease. Despite significant advances in our
78 understanding of MDC1A pathophysiology, currently, there is no cure.
79 Due to the genetic nature of the disease, gene therapy is a promising treatment option
80 for MDC1A. The large size of *LAMA2* transcript, however, presents a challenge with
81 respect to gene delivery. We have recently overcome this challenge by using
82 CRISPR/Cas9 technology to correct a mutation in *Lama2* gene *in vivo* ⁴. We focused on
83 *dy^{2j}/dy^{2j}* mouse model, which harbors a splice site mutation in *Lama2* causing
84 spontaneous exon skipping and truncation of N-terminal domain of the protein ⁵. We
85 developed an exon inclusion strategy to correct the splice mutation, leading to
86 restoration of full-length *Lama2*. This study established the first direct correction of the
87 primary genetic defect underlying MDC1A in an *in vivo* model.
88 To date, there are over 350 reported pathogenic nonsense-, missense-, splice site- and
89 deletion mutations in the *LAMA2* gene. Given the variety of MDC1A-causing genomic
90 alterations, CRISPR/Cas9-mediated gene editing strategies would require design and
91 thorough analysis of multiple sgRNAs specific for each individual mutation. Moreover,
92 safety concerns regarding CRISPR/Cas9's potential mutagenic nature and the presence
93 of off-target effects after gene editing remain, which together may prove to be
94 challenging from a safety and regulatory point-of-view. In contrast, the attenuation of
95 disease pathogenicity by targeted modulation of disease modifier gene expression would
96 be a potentially safer alternative and beneficial to all individuals with MDC1A.
97 One of the strongest reported disease modifiers for MDC1A is Laminin- α 1 protein, which
98 is structurally similar to Laminin- α 2 (**Fig. 1a**). However, Laminin- α 1 is not expressed in
99 skeletal muscles or Schwann cells. A series of studies previously demonstrated that
100 transgenic expression of *Lama1*, encoding Laminin- α 1, rescued both myopathy and

101 peripheral neuropathy in dy^{2j}/dy^{2j} ⁶ and dy^{3K}/dy^{3K} ^{2,7-10}; the latter also showed increased
102 lifespan. Although these studies firmly established compensatory function of Laminin- α 1
103 in MDC1A, utilization of this modifier as a postnatal gene therapy is hampered by the
104 size of *Lama1* cDNA, which exceeds the 4.7 kb packaging capacity of AAV vectors.
105 Advances in CRISPR/Cas9 technologies have provided opportunities for regulating gene
106 expression and creating epigenetic alterations without introducing DNA double-strand
107 breaks (DSBs); commonly termed CRISPR transcriptional activation/inhibition system.
108 The strategy utilizes nuclease-deficient Cas9 (dCas9), which is unable to cleave DNA
109 due to mutations within the nuclease domains, but still retains the ability to specifically
110 bind to DNA when guided by a single guide RNA (sgRNA)^{11,12}. Using the originally
111 described *S. pyogenes* (*Sp*) dCas9 fused to multiple copies of the VP16 transcriptional
112 activator, our group and others have demonstrated utilization of the CRISPR/dCas9
113 system to upregulate expression of modifier genes *in vitro*¹¹⁻¹⁴. A major challenge for *in*
114 *vivo* applications lies in the large size of *SpdCas9* and its transcriptional activator fusion
115 derivatives that exceed AAV genome packaging capacity. To accommodate this
116 limitation, we sought to adapt the transcriptional upregulation system and utilize a
117 significantly smaller Cas9 protein derived from *S. aureus* (*Sa*)¹⁵ to upregulate MDC1A
118 modifier *Lama1*. We hypothesized that CRISPR/dCas9-mediated transcriptional
119 upregulation of *Lama1* would be sufficient to compensate for the lack of *Lama2* and
120 ameliorate disease phenotypes in dy^{2j}/dy^{2j} mice.
121 First, we mutagenized *SaCas9* endonuclease catalytic residues (D10A, N580A) to
122 create *SadCas9* and then fused it to transcriptional activators VP64 (four copies of
123 VP16) on both N- and C-termini (**Fig. S1**). We tested the ability of the system, denoted
124 as *SadCas9*-2xVP64, to upregulate the expression of minCMV-driven *tdTomato* gene in
125 293T cells¹⁶. In the absence of the *SadCas9*-2xVP64, the expression of *tdTomato* was
126 undetectable due to the low baseline activity of minCMV promoter (**Fig. S1a, b**). In the
127 presence of *SadCas9*-2xVP64 in combination with an sgRNA targeting the minCMV
128 locus, we observed high *tdTomato* fluorescence signal (**Fig. S1c, d**), indicating the
129 general applicability of this system to modulate expression of a gene of interest.
130 Subsequently, we tailored the system to upregulate *Lama1* expression and designed five
131 sgRNAs, denoted as g1 to g5, within the 500 nucleotides region immediately upstream
132 of the *Lama1* transcription start site (**Figs. 1b, c**). When co-expressed with *SadCas9*-
133 VP64 in C2C12 murine myoblasts, 3 out of 5 sgRNAs, namely g1, g2, and g5
134 consistently induced significant increase of *Lama1* transcript expression (**Figs. 1d, e**).

135 Although all sgRNAs were designed to target a chromatin-accessible region derived
136 from DNase1 hypersensitivity- and assay for transposase-accessible chromatin (ATAC-
137 Seq) sites (**Fig. 1b**), g3 and g4 failed to increase expression of *Lama1* above the basal
138 level. This corroborates previously reported findings that chromatin accessibility is not a
139 reliable predictor of successful gene activation^{12,17,18}. Nonetheless, the sgRNA closest to
140 the transcription start site, g1, and the combination of the three most optimum sgRNAs
141 (g1, g2, g5) resulted in a robust increase in Lama1 protein expression in *dy^{2j}/dy^{2j}*-derived
142 myoblasts (**Figs. 1f, 1g**), warranting further investigation *in vivo*.

143 We then treated 3-week-old *dy^{2j}/dy^{2j}* mice with an AAV9 carrying FLAG-tagged
144 SadCas9-2xVP64 in the absence of sgRNA (no guide) or with g1 (single guide) or a
145 combination of g1, g2 and g5 (three guides) (**Fig. 2a**). Due to the packaging capacity of
146 the AAV, the dCas9-2xVP64 and the three guides were split into two vectors (**Fig. 2a**).
147 Each mouse received a single intramuscular injection of 7.5×10^{11} viral genomes of
148 AAV9, which was doubled to 1.5×10^{12} viral genomes total for the three guide cohort, in
149 the right *tibialis anterior* (TA) and was sacrificed 4 weeks post injection. FLAG
150 expression was detected by western blot in all SadCas9-2xVP64-injected right TA
151 muscles, however, only those injected with guide-containing constructs showed Lama1
152 upregulation (**Fig. 2b**). Similarly, immunofluorescence staining revealed sarcolemmal
153 expression of Lama1 (**Fig. 2c**, upper), indicating proper protein localization.
154 Furthermore, H&E staining exhibited considerably improved muscle architecture (**Fig.**
155 **2c**, lower) in the single- and three guide treatment groups, as compared to the no guide
156 controls.

157 Next, we sought to investigate whether upregulation of *Lama1* could be achieved
158 systemically *in vivo* and, if administered into pre-symptomatic neonatal *dy^{2j}/dy^{2j}* mice,
159 would prevent the manifestation of dystrophic pathophysiology and paralysis. AAV9
160 particles carrying either no guide or a combination of three guides were injected into the
161 temporal vein of 2-day-old (P2) *dy^{2j}/dy^{2j}* mice (**Fig. 3a**). Seven weeks post injection, the
162 animals that received the three guides treatment showed an absence of classical
163 hindlimb contracture, unlike the control group (**Fig. 3b; Supplementary videos 1 and**
164 **2**). Western blot, immunofluorescence and H&E staining of TA and gastrocnemius
165 muscles demonstrated robust expression of Lama1 on the sarcolemmal membrane (**Fig.**
166 **3c, 3d**), leading to ~50% reduction of fibrosis (**Figs. 3e, 3f, S2**).

167 We subsequently examined the ability of *Lama1* upregulation to reverse established
168 muscular and peripheral nerve dysfunctions by initiating the treatment at 3 weeks of age,

169 when paralysis was already apparent^{19,20} (**Fig. 4a**). We first tested three different doses,
170 ranging from 7.5×10^{10} to 3×10^{11} viral genome/gram of mouse per AAV9, which was
171 doubled for the three guide cohorts due to the utilization of two vectors, and found that
172 the highest dose resulted in homogeneous Lama1-positive fibers (**Fig. S3a**), significant
173 improvement of muscle function and mobility (**Figs. S3b, S3c**). Longitudinal
174 measurement of animal mobility and stand-up activity in a non-invasive open field
175 activity assay showed significant difference between no guide and three guides-treated
176 mice starting at 5 and 6 weeks old, respectively, which was sustained over time (**Figs.**
177 **4b, 4c**). Furthermore, specific tetanic force, which measures the aggregate torque
178 produced by the dorsi flexor muscles, was also improved in the three guides-treated
179 mice (**Fig. 4d**). In line with this finding, we observed a significant increase in nerve
180 conduction velocity, which indicates restoration of the myelination defect and contributes
181 to neuromuscular functionality (**Fig. 4e**). The absence of paralysis in the hind limbs and
182 markedly improved movement of the mice were evident at the end of the treatment
183 regimen (**Supplementary videos 3, 4**).

184 Molecular analysis of the treated mice revealed strong Lama1 expression by
185 immunostaining and western blot (**Figs. 4f, 4g, S4**), which was accompanied by
186 normalization of $\alpha 4$ chain of the laminin subunit (**Figs. S5, S6**)⁶, significant improvement
187 in muscle histopathology (**Fig. 4h**) and approximately 50% reduction in the fibrotic area
188 (**Fig. 4i**) compared to the no guide control group. There was a trend towards larger fibers
189 in the treated mice, although it did not reach statistical significance due to the large
190 variation between animals (**Fig. 4j**). In addition, upregulation of Lama1 was also
191 observed in the endoneurium of sciatic nerves and resulted in restoration of myelination
192 defect (**Figs. 4k, S7**), supporting the improvement of nerve conduction velocity and lack
193 of paralysis in the mice (**Fig. 4e, Supplementary videos 3, 4**). Quantification of the AAV
194 genome copy number revealed accumulation of most of the viral genome in the liver,
195 which is expected from intravenous delivery. Nevertheless, approximately 1.11 ± 0.4 and
196 34.1 ± 4.3 copies/diploid genome of the viral genome were detected in the sciatic nerves
197 and skeletal muscles, respectively (**Fig. S8**). Remarkably, even relatively low
198 transduction efficiency in sciatic nerves was sufficient for functionally significant
199 upregulation of Lama1 expression.

200 Finally, we investigated the genome wide effects of CRISPR/dCas9-mediated Lama1
201 upregulation by performing RNA-sequencing on quadriceps muscles isolated from mice
202 treated with AAV9 carrying no guide and three guides (**Figs. S9, S10, Supplemental**

203 **Tables 1-3**). Age-matched wildtype and dy^{2j}/dy^{2j} mice served as controls. We observed
204 a 3.6- \log_2 fold upregulation of *Lama1* (defined by a false discovery rate, FDR <0.05)
205 when comparing the mice treated with AAV9 carrying no guide and three guides (**Fig.**
206 **S9a**). The transcriptional change was even higher at 9- \log_2 fold when comparing
207 untreated dy^{2j}/dy^{2j} with three guide-treated dy^{2j}/dy^{2j} (**Fig. S9b, S9c**). Hierarchical
208 clustering between groups revealed clustering between wildtype and three guides,
209 whereas the untreated cohort was clustered together with no guide-treated mice (**Figs.**
210 **S9d, S10**). We also computationally predicted 704 potential off-target binding sites for
211 the three sgRNAs targeting *Lama1* promoter in the mouse genome, selected based on
212 the presence of a 6bp PAM-proximal seed sequence and fewer than ten total
213 mismatches to the cognate target sequence (**Supplemental Tables 4-5**). None of the
214 top 100 genes contained a predicted off-target site within 60 kilobases of the gene body,
215 with the average distance from off-target site to the gene body being 2.2 megabases.
216 Taken together, our results provide strong evidence of the robustness and durability of
217 CRISPR/dCas9-mediated *Lama1* upregulation for the treatment of MDC1A. Additionally,
218 we show the therapeutic promise of the strategy for reversal of dystrophic feature in
219 skeletal muscle and peripheral neuropathy in dy^{2j}/dy^{2j} mouse model of MDC1A, which
220 ultimately halts progression of the disease, without any confounding off-target effects.
221

222 One challenge in developing a therapy for MDC1A is that the heterogeneity of mutations
223 often leads to variable disease severity and progression. Therefore, there is an urgent
224 need to develop a universal, mutation-independent strategy that provides a treatment
225 approach for all patients with MDC1A. Our study establishes a framework in which
226 CRISPR/dCas9 transcriptional upregulation of a disease modifier gene, such as *Lama1*,
227 ameliorates disease symptoms *in vivo* and has the potential to be applied to all MDC1A
228 patients, irrespective of their mutations.

229 Advances have been made towards elucidating MDC1A pathogenesis due to the
230 availability of several mouse models with absent or reduced *Lama2* expression. Yet, an
231 important question in the development of therapeutics and clinical trials in MDC1A is the
232 reversibility of symptoms caused by muscle fibrosis and nerve abnormalities. This issue
233 has been challenging to address in patients²¹, however, the ability to modify gene
234 expression in postnatal animals allowed us to address this question and begin to
235 investigate the therapeutic window of intervention.

236 We have previously demonstrated that an early intervention using CRISPR/Cas9-
237 mediated correction of a splicing defect resulted in robust *Lama2* restoration and
238 prevention of disease manifestation⁴. Here we showed that upregulation of *Lama1*,
239 when initiated at pre-disease-onset, leads to similar prevention. Importantly, when the
240 therapeutic intervention was initiated at older age, significant rescue of the phenotypes
241 was attainable, indicating that post-symptomatic treatment provides a significant benefit
242 in the *dy^{2j}/dy^{2j}* mouse model.

243 In addition to *Lama1* upregulation described in this study, a number of disease modifying
244 strategies are currently being explored in MDC1A animal models, including treatment
245 with miniaturized agrin²²⁻²⁴ and laminin- α 1 LN-domain nidogen-1 (α LNNd)²⁵⁻²⁷. While
246 the efficacy of α LNNd has only been explored in transgenic mice, AAV-mediated delivery
247 of mini agrin has been shown to normalize most histopathological parameters in skeletal
248 muscle, and improve myelination and regeneration of Schwann cells of the peripheral
249 nerves^{22,24}. Despite the observed phenotypic improvement, the mini agrin-treated mice
250 still have a lower survival rate compared to wild-type animals expressing full-length
251 agrin, suggesting the potential shortcoming of the shortened version of agrin, which may
252 be overcome by its full-length form in native glycosylation state²⁵. It is important to note
253 that many preclinical studies in MDC1A were carried out in the more severe *dy^W/dy^W*
254 mouse model. Therefore, as a follow up on our study, it will be important to evaluate our
255 approach in the *dy^W/dy^W* mice to assess critical parameter such as survival, which is not

256 possible in the dy^{2j}/dy^{2j} mouse model due to its near-normal life span. Overall, our
257 approach in combining the CRISPR/dCas9-mediated transcriptional upregulation and
258 AAV9 as a delivery vehicle can be translated to many other disease modifiers, such as
259 agrin, as well as conditions where modulation of disease modifiers is required within
260 both skeletal muscles and peripheral nerves.

261 In fact, neuromuscular disorders have provided excellent examples to demonstrate the
262 role of disease modifiers (recently reviewed in ²⁸). Beyond MDC1A, several studies have
263 demonstrated that upregulation of *Lama1* stabilizes the sarcolemmal membrane in
264 dystrophin-deficient mouse models ²⁹. The most advanced approach is via delivery of
265 Laminin-111 protein, although the efficacy remains low and the need to produce a large
266 amount of bioactive protein is challenging ²⁹. In addition, the utilization of CRISPR/dCas9
267 system to upregulate *Lama1* in *mdx* mice has been achieved locally via electroporation,
268 which is not easily translatable into clinical settings ³⁰. Our strategy of employing AAV-
269 mediated *S. aureus* dCas9 to upregulate *Lama1 in vivo* may be tested further as a
270 potential therapy in the context of Duchenne muscular dystrophy.

271 In addition, since the CRISPR/dCas9-mediated transcriptional modulation acts directly
272 on the endogenous locus, it may be used in conjunction with a mutation-correction
273 approach where the level of restoration of the defective gene is suboptimal, therefore
274 necessitating further amplification to reach therapeutic efficacy ^{4,31-36}.

275 A very recent study by Liao *et al* described utilization of the CRISPR/Cas9 system to
276 recruit MCP:P65:HSF1 transcriptional activation complex to induce expression of target
277 genes in skeletal muscle, kidney and liver tissues ¹⁸. This resulted in phenotypic
278 augmentation such as enhanced muscle mass and substantial improvement in disease
279 pathophysiology, thereby highlighting the feasibility of using CRISPR/dCas9-mediated
280 transcriptional activation as a possible therapeutic modality. However, their study relied
281 almost exclusively on a Cas9-expressing transgenic mouse model or local intramuscular
282 treatments, and therefore it is difficult to extrapolate the efficacy of this strategy to
283 disease-relevant models. In contrast, we successfully demonstrated robust upregulation
284 of *Lama1* after systemic delivery of therapeutic components in a relevant mouse model
285 of disease that does not constitutively express Cas9.

286 Finally, the modular nature of the CRISPR/dCas9 system can be utilized to not only to
287 upregulate, but also to downregulate target gene expression. The latter can be achieved
288 by coupling dCas9 with transcriptional repressor such as Kruppel-associated box
289 (KRAB) ^{17,37}. A very recent study described that following sarcolemmal injury, the muscle

290 membrane resealing process is greatly improved upon the deletion of Osteopontin,
291 which acts in a concerted fashion with protective modifiers such as Latent TGF- β binding
292 protein (LTBP4) and Annexins 1 and 6^{38,39}. The combinatorial effects of such modifiers,
293 whether they are additive, synergistic or even opposing in action, represent a new
294 paradigm for lessening disease phenotypes. A foreseeable application of
295 CRISPR/dCas9-mediated modulation is in the upregulation of protective disease
296 modifier genes, such as Lama1 or LTBP4, with concurrent downregulation of detrimental
297 genes, such as Osteopontin, providing a combinatorial therapeutic approach.
298 In summary, our study establishes a framework to utilize CRISPR/dCas9 to modulate
299 gene expression of disease modifiers that should be considered as a mutation-
300 independent therapeutic strategy not only to MDC1A, but also to various other inherited
301 and acquired diseases.

302 **Methods**

303

304 **Engineering of activation constructs**

305 A fragment containing a catalytically inactive *SaCas9* coupled to two flanking VP64
306 transactivator domains was synthesized by BioBasic Canada and cloned into pX601
307 (Addgene 61591) using *AgeI* and *EcoRI* directional cloning to generate 3XFLAG-VP64-
308 *SadCas9* (D10A/N580A)-NLS-VP64 plasmid (**Figs. 2a, S11, Supplemental Table S6**).
309 Each sgRNA (**Supplemental Table S6**) was subsequently introduced using *BsaI*
310 directional cloning. To generate the three guides only construct (**Fig. 2a**), a fragment
311 containing three repetitive regions of U6 promoter and *S. aureus* guide scaffold was
312 assembled, with short linkers in between each region (BioBasic Canada). The fragment
313 was cloned into *KpnI* and *NotI* sites of a pX601-derivative plasmid.

314

315 **Cell Culture**

316 Primary myoblasts were isolated from the Extensor Digitorum Longus (EDL) Muscle of
317 *dy^{2J}/dy^{2J}* mice, as previously described⁴⁰ and maintained in DMEM supplemented with
318 1% chicken embryo extract (GeminiBioscience), 10% horse serum, 1%
319 penicillin/streptomycin and 1% L-glutamine (all from Gibco, unless indicated otherwise).
320 HEK293 and C2C12 cells were maintained in DMEM supplemented with 10% FBS, 1%
321 penicillin/streptomycin and 1% L-glutamine (all from Gibco). All cells were maintained at
322 37°C with 5% CO₂.

323 Transfection of HEK293T cells was performed as previously described². C2C12 and
324 *dy^{2J}/dy^{2J}* cells were transfected in 12-well plates using the Neon Transfection System
325 (Invitrogen). 400,000 cells were electroporated with 1.5 µg of DNA utilizing optimization
326 program 16 (pulse voltage: 1400V, pulse width: 20ms, pulse number: 2). Cells were
327 grown for 72 hours, after which RNA or protein was subsequently collected for protein
328 analysis and guide screening.

329

330 **Animals, virus production and injections**

331 *dy^{2J}/dy^{2J}* mice were purchased from the Jackson Laboratory and maintained in the
332 Toronto Center for Phenogenomics. Both male and female were used in the analyses.
333 All animal experiments were performed according to Animal Use Protocol number 20-
334 0305. *SadCas9*-2xVP64, single guide and three guides plasmids (**Fig. 2a,**
335 **Supplemental Table S6**) were packaged into AAV9 vectors by Vigene Biosciences as

336 previously described³. For intramuscular and temporal vein injection into neonatal pups,
337 the dose of 7.5×10^{11} viral genomes each was used. Due to the limitation in packaging
338 capacity, two AAVs were needed for the three guides cohort (**Fig. 2a**), therefore the total
339 virus injected was 1.5×10^{12} viral genomes per animal. Injection volume was brought to
340 50 μ l with 1XPBS (Gibco).

341 For the tail vein injection in young, 3 week old mice, three different doses were initially
342 tested: 7.5×10^{10} , 1.5×10^{11} and 3×10^{11} viral genomes per gram of mouse (**Fig. S3**).

343 Similar to the intramuscular and temporal vein injections, two AAVs were needed for the
344 three guides cohort, therefore the total dose used in experiments described in **Figs. 4,**
345 **S4-S10** was 6×10^{11} viral genomes per gram of mouse. Injection volume was brought to
346 100 μ l with 1XPBS (Gibco).

347

348 **RNA isolation, guide screening and RT-PCR**

349 RNA was isolated from cultured cells and mouse tissue sections, and cDNA synthesis
350 was performed as previously described³. PCR amplification was utilized to assess the
351 efficiency of each guide in upregulating *Lama1* expression using a primer in *Lama1* exon
352 55 (RDC 1919) and a second primer spanning the junction of exons 55 and 56 (RDC
353 1920). Sequences are listed in **Supplemental Table S6**.

354 qPCR utilizing Fast SYBR green Master Mix (Qiagen) on a Step One Plus Real Time
355 PCR (Applied Biosystems) was performed. *Lama1* expression was analyzed using a
356 primer in *Lama1* exon 55 (RDC 1919) and one spanning the junction of exons 55 and 56
357 (RDC 1920). Primers against endogenous Gapdh (RDC 345 and 346) were used as an
358 internal control. $\Delta\Delta$ Ct was analyzed to assess fold changes between treated and
359 untreated samples.

360

361 **Protein Isolation and western blot**

362 Protein was isolated from *dy^{2j}/dy^{2j}* myoblasts and C2C12 cells by adding 150 μ l of a 1:1
363 part solution of RIPA homogenizing buffer (50-mM Tris HCl pH 7.4, 150-nM NaCl, 1-mM
364 EDTA) and RIPA double-detergent buffer (2% deoxycholate, 2% NP40, 2% Triton X-100
365 in RIPA homogenizing buffer) supplemented with protease-inhibitor cocktail (Roche).
366 Cells were subsequently scraped from the bottom of each well, collected and incubated
367 on ice for 30 min. Cells then centrifuged at 12000xg for 15 min at 4°C and the
368 supernatant was collected and stored at -80°C. Protein from mouse tissue sections was
369 collected as previously described³. Whole protein concentration was measured using

370 Pierce BCA protein assay kit according to the manufacturer's protocol (Thermo Fisher
371 Scientific). Western blot was performed as previously described³. Primary antibodies
372 used were rabbit Anti-LN α 1 E3 (a gift from Dr. Peter Yurchenco, 0.6 μ g/ml), mouse
373 monoclonal M2 anti-Flag (Sigma Aldrich F1804, 1:1000) and rabbit polyclonal anti-
374 GAPDH (Santa Cruz sc-25778, 1:5000).

375 **Immunofluorescence and H&E staining**

376 Muscles and nerves were sectioned at 8 μ m thickness and processed for
377 immunofluorescence analyses according to standard procedures. Antibodies used for
378 immunofluorescence staining were rat monoclonal against Laminin α 1 (mAb200,
379 Durbeej Lab, 1:20), α 2 (4H8-2, Sigma, 1:500), γ 1 chain (clone A5, Thermo Fisher
380 Scientific), rabbit polyclonal against Laminin α 4 chain (kindly provided by Dr. Sasaki),
381 mouse monoclonal against NF-H (Biolegend SMI 31, 1:1000), goat polyclonal anti-rat
382 Alexa Fluor 555 (Thermo Fisher Scientific, 1:250) and goat polyclonal anti-mouse Alexa
383 Fluor 488 (Thermo Fisher Scientific, 1:250). H&E staining was performed as previously
384 described⁴. Both immunofluorescence and H&E slides were scanned with the 3Dhistech
385 Panoramic 250 Flash II digital scanner and analyzed with CaseViewer software, with
386 the exception of **Figs. S5, S6**, which were analyzed with a Zeiss Axioplan fluorescence
387 microscope (Carl Zeiss) and images were captured using an ORCA 1394 ER digital
388 camera (Hamamatsu Photonics) and Open Lab software version 4 (Improvision).

389

390 **Toluidine blue staining and electron microscopy**

391 Freshly isolated mouse sciatic nerves were halved and fixed in a solution of 2%
392 paraformaldehyde and 2.5% glutaraldehyde in 0.1M sodium cacodylate buffer until
393 further use. For embedding, the specimens were rinsed with the 0.1M sodium
394 cacodylate buffer, post-fixed in 1% osmium tetroxide in the washing buffer, dehydrated
395 in a graded ethanol series followed by propylene oxide, and embedded in Quetol-Spurr
396 resin overnight at 65⁰C. Sections of 90nm thickness were cut on a Leica EM UC7
397 ultramicrotome, stained with uranyl acetate and lead citrate, and imaged on a FEI Tecnai
398 20 electron microscope at 4400-, 10,000-, and 44,000X magnifications. The same 90nm
399 sections were stained with toluidine blue and imaged on a Leica DM-2000. All reagents
400 were purchased from Electron Microscopy Sciences. Quantification of myelin thickness
401 was measured using ImageJ from at least 14 random axons per field (at least 5 fields
402 per animal)⁴¹.

403 **Open field and *in vivo* muscle force assays**

404 Open field activity test and assessment of *in vivo* muscle force were performed on tail
405 vein injected cohorts at the Lunenfeld-Tanenbaum Research Institute's Centre for
406 Modeling Human Disease Mouse Phenotyping Facility. For the open field test, mice
407 were placed in the frontal center of a transparent Plexiglas open field (41.25 cm × 41.25
408 cm × 31.25 cm) illuminated by 200 lx. A trained operator, who is unaware of the nature
409 of the projects and treatments, performed experiments. The VersaMax Animal Activity
410 Monitoring System recorded vertical activities and total distance travelled for 20 minutes
411 per animal.

412 *In vivo* muscle contraction test was performed using 1300A: 3-in-1 Whole Animal
413 System and analyzed using Dynamic muscle control/analysis (DMC/DMA) High
414 throughput software suite (Aurora Scientific). The mice were anaesthetised with
415 intraperitoneal injection of ketamine/xylazine cocktail at 100 mg/kg and 10 mg/kg of body
416 weight, respectively. Contractile output was measured via percutaneous electrodes that
417 stimulate specific nerves innervating the plantar flexors. Specific tetanic force (200 ms of
418 0.5-ms pulses at 125 Hz) was recorded and corrected to body weight.

419

420 **Nerve conduction velocity**

421 Mice were anesthetized with urethane (1.2 mg/g i.p.) and underwent a tracheotomy to
422 maintain their airway but were not artificially ventilated. Core body temperature was
423 maintained at 34-36.5°C using a feedback-controlled heating pad (TR-200; Fine Science
424 Tools). The sciatic nerve was exposed at two locations via incisions (~15 mm) above the
425 left knee (site #1) and along the sacral region of the vertebral column (site #2). After
426 separating the nerve from adjacent tissue, a bipolar hook electrode was applied to the
427 nerve at each site. Each electrode comprised two chlorided silver wires (0.01" diameter,
428 A-M systems) placed ~1 mm apart and bent at the tip to form hooks, and attached to a
429 stimulator (Model DS3, Digitimer Ltd). Stimulating electrodes were insulated from
430 underlying tissue using a small piece of plastic paraffin film. Stimulus duration was fixed
431 at 20 µs and current intensity was varied. Stimulus timing was controlled by computer
432 using a Power1401 computer interface and Signal v5 software (Cambridge Electronic
433 Design, CED). The compound muscle action potential (CMAP) was recorded using
434 needle electrodes (~30 G, BD *PrecisionGlide*™), one inserted into the gastrocnemius
435 muscle and the other (reference) electrode inserted into the Achilles tendon. The CMAP
436 signal was amplified, low-pass filtered at 10 Hz and high-pass filtered at 1 kHz (DAM 80,

437 World Precision Instruments), and digitized at 40 kHz using the Power1401 and Signal
438 v5 software (CED). To calculate conduction velocity (CV) from CMAP responses, the
439 sciatic nerve was stimulated at just-maximal intensity (beyond which there is no change
440 in CMAP amplitude or latency) three times at site #1 and again three times at site #2.
441 Nerve conduction velocity was calculated as the difference between average CMAP
442 latencies for each stimulation site divided by the length of nerve (7.5-10 mm) separating
443 the sites.

444

445 **Vector genome quantification**

446 Evaluation of AAV genome distribution was performed as previously published⁴² with a
447 few modifications. Genomic DNA was extracted from tibialis anterior, sciatic nerve, and
448 liver of treated mice using Qiagen Blood and Tissue Kit. 90 ng of DNA was amplified
449 using primers located in between the two inverted tandem repeats (ITRs) (RDC 1687,
450 RDC 1679, **Supplemental Table S7**) using Fast SYBR green master mix (Qiagen) on a
451 Step One Plus Real Time PCR (Applied Biosystems). The Ct value of each reaction was
452 converted to viral genome copy number by interpolating against the copy number of
453 standard curve of a known plasmid containing the sgRNA cassette (RDC 362). The
454 amount of DNA input (90 ng per tissue) was used as a conversion factor to diploid
455 genome (7 picogram DNA = 1 diploid genome).

456

457 **RNA-Sequencing**

458 Total RNA was isolated from quadriceps muscles using RNeasy kit (Qiagen) and
459 quantified using Qubit RNA HS assay (Thermo Fisher Scientific). RNA-Sequencing was
460 performed by the Centre for Applied Genetics in Toronto using the Illumina HiSeq 2500
461 system, producing 120bp paired-end reads. Raw transcript reads were aligned to the
462 GRCm38 mouse genome (mm10) using HISAT2⁴³. HTSeq was used to determine the
463 absolute number of read counts for each gene⁴⁴. Only genes with at least 1 read per
464 million in at least three replicates were kept for downstream analysis. Normalization and
465 differential expression analysis was completed using the R packages limma, v3.36.3 and
466 edgeR, v.3.22.3⁴⁵. Differentially expressed genes were defined as genes with a more
467 than twofold change and adjusted $P < 0.05$. Off-target analysis was conducted using a
468 list of 704 computationally predicted using Cas-OFFinder⁴⁶. Using the Bedtools suite
469 “closest” function, each of the top 100 differentially expressed genes was matched to the

470 nearest off-target loci to determine the shortest distance from off-target loci to
471 differentially expressed gene body.

472

473 **Statistical Analysis**

474 GraphPad Prism (GraphPad software) was utilized to preform all statistical analyses.
475 Two-tailed Student' t-tests to evaluate statistical significance between two groups was
476 preformed. Significance was considered to be $P < 0.05$.

477

478 **Data availability**

479 The authors declare that the main data supporting the findings of this study are available
480 within the article and its Supplementary Information files. Extra data are available from
481 the corresponding authors upon request.

482

483 **Acknowledgements**

484 The Cohn lab members are gratefully acknowledged for the technical support and critical
485 input in this study. We thank P. Yurchenco (Rutgers University) for providing critical
486 reagents in this study, C. Rand (Aurora Scientific), I. Vukobradovic (Clinical Phenotyping
487 Core, Centre for Modeling Human Disease), R. Smith (Prescott Lab) for assistance with
488 functional and behavioral studies, D. Holmyard (Nanoscale Biomedical Imaging Facility)
489 for electron microscopy analysis and S. Pereira (The Centre for Applied Genomics) for
490 genomic data acquisition.

491 This work was supported by AFM-Telethon, Cure CMD, Muscular Dystrophy Association
492 (to D.U.K), Rare Disease Foundation Microgrant (to P.S.B. and S.E.), SickKids
493 Restracom (to S.E.), CIHR Summer Studentship (to R.M.), Natural Sciences and
494 Engineering Research Council of Canada, Canadian Institute for Health Research,
495 SickKids Foundation and R.S. McLaughlin Foundation Chair in Pediatrics (to R.D.C).

496

497 **Author contributions**

498 D.U.K., E.A.I., R.D.C. conceived the study, D.U.K., P.S.B., S.E., D.A.B., K.I.G., K.L.,
499 E.H., R.K., K.M.P., R.M., performed the experiments, D.A.B., K.I.G., M.D., S.A.P.
500 provided critical reagents, D.U.K., P.S.B, S.E., D.A.B, K.I.G, S.A.P., E.A.I, R.D.C.
501 analyzed data, D.U.K, E.A.I., R.D.C. supervised the study, D.U.K. wrote the manuscript
502 with inputs from the other authors. All authors provided feedback and agreed on the final
503 manuscript.

504

505
506

Figure legends

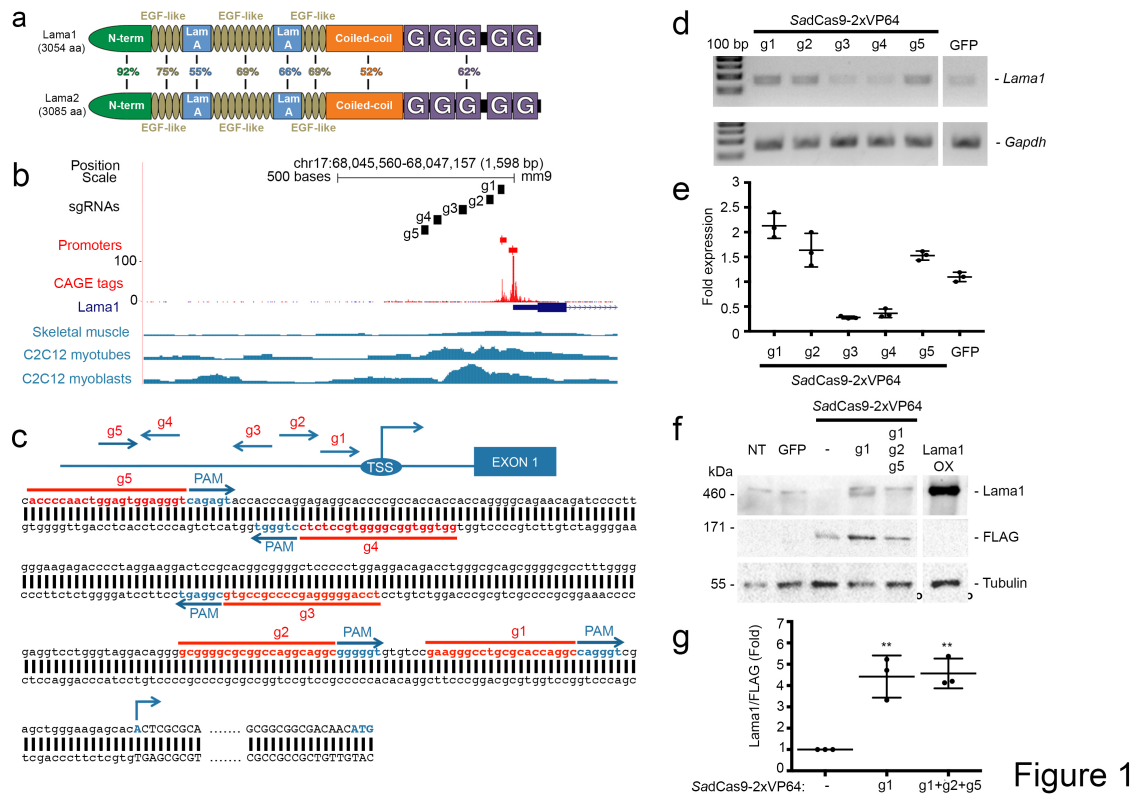


Figure 1

507

508 **Fig. 1. SadCas9-2xVP64-mediated upregulation of *Lama1* in vitro.** (a) Lama1 and
 509 Lama2 protein alignment. Total amino acid (aa) and percentage similarity between each
 510 domain are indicated. (b) Analyses of Lama1 proximal promoter. Five sgRNAs (g1-g5)
 511 were designed in the proximal promoter region of Lama1 immediately upstream of the
 512 transcription start site (TSS), as indicated by CAGE tags (red). Chromatin accessibility in
 513 skeletal muscle tissue and cells (retrieved using Digital DNase footprinting and ATAC-
 514 Seq) are shown in blue. Data were plotted according to positions from the UCSC
 515 Genome Browser. (c) Positions of the five sgRNAs relative to *Lama1* TSS. Arrowheads
 516 indicate the direction of each sgRNA. Sequences of each sgRNA (red) are immediately
 517 downstream (5') of *Sa* PAM sequences (NNGRRT) (in blue). ATG indicates translation
 518 start site. (d-e) C2C12 myoblasts were transfected with a plasmid containing SadCas9-
 519 2xVP64 and the corresponding sgRNA(s) targeting *Lama1*, and 72 hours post-
 520 transfection, analyzed by (d) RT-PCR and (e) qRT-PCR. Single and combination of
 521 optimal sgRNAs were transfected into *dy^{2j}/dy^{2j}* myoblasts and Lama1 protein expres-
 522 sion was assessed by western blot (f). FLAG expression serves as transfection control and
 523 used to (g) normalize Lama1 upregulation by densitometry analysis. Data are presented

524 as mean \pm standard deviation from at least three independent experiments. Statistical
 525 analysis was performed using Student's *t*-test. ** $P < 0.01$.

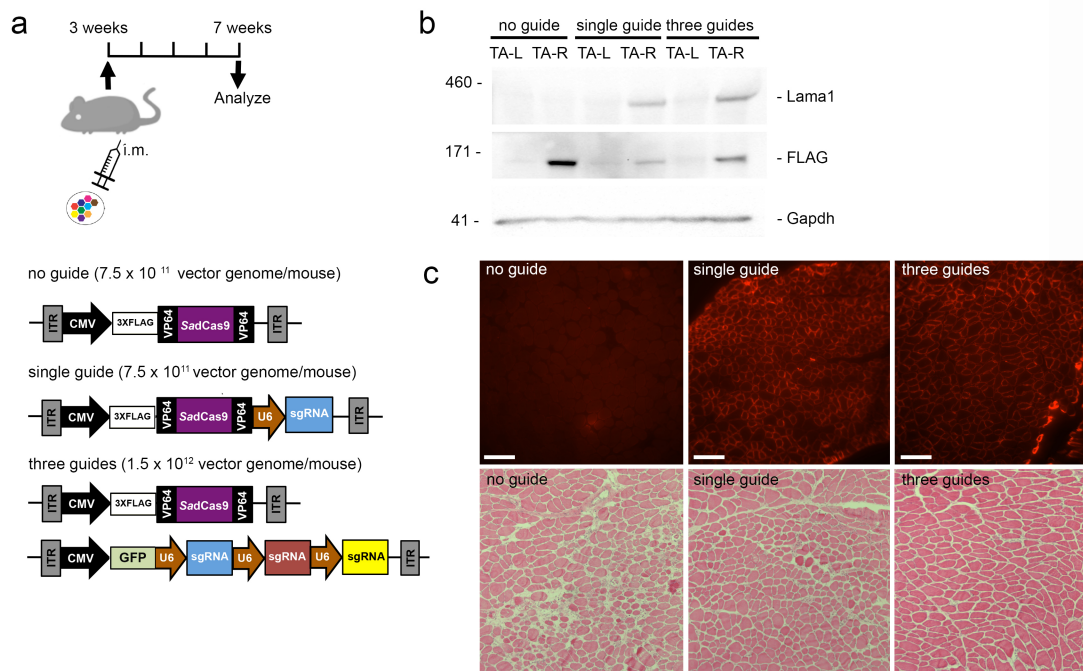


Figure 2

526

527 **Fig. 2. Upregulation of Lama1 in tibialis anterior (TA) muscles of dy^{2j}/dy^{2j} mice**
 528 **following intramuscular administration.** (a) Right TA muscles of 3-week old dy^{2j}/dy^{2j}
 529 mice were injected with AAV9-carrying no guide (n=4; 7.5×10^{11} viral genomes), single
 530 guide (n=4; 7.5×10^{11} viral genomes) or three guides (n=4; split into two vectors, thus
 531 total dose was $2 \times 7.5 \times 10^{11}$ viral genomes). ITR: Inverted Terminal Repeats. CMV and U6
 532 promoters are depicted in arrows. Left TA muscles serve as control. (b) Western blot
 533 analysis on Lama1, FLAG-tagged SadCas9, and Gapdh expression. (c)
 534 Immunofluorescence (upper) and H&E (lower) stainings on cross-sections of right TA
 535 muscles from each treatment group. Scale bar: 50 μ m. Representative images from one
 536 animal per treatment group are shown.

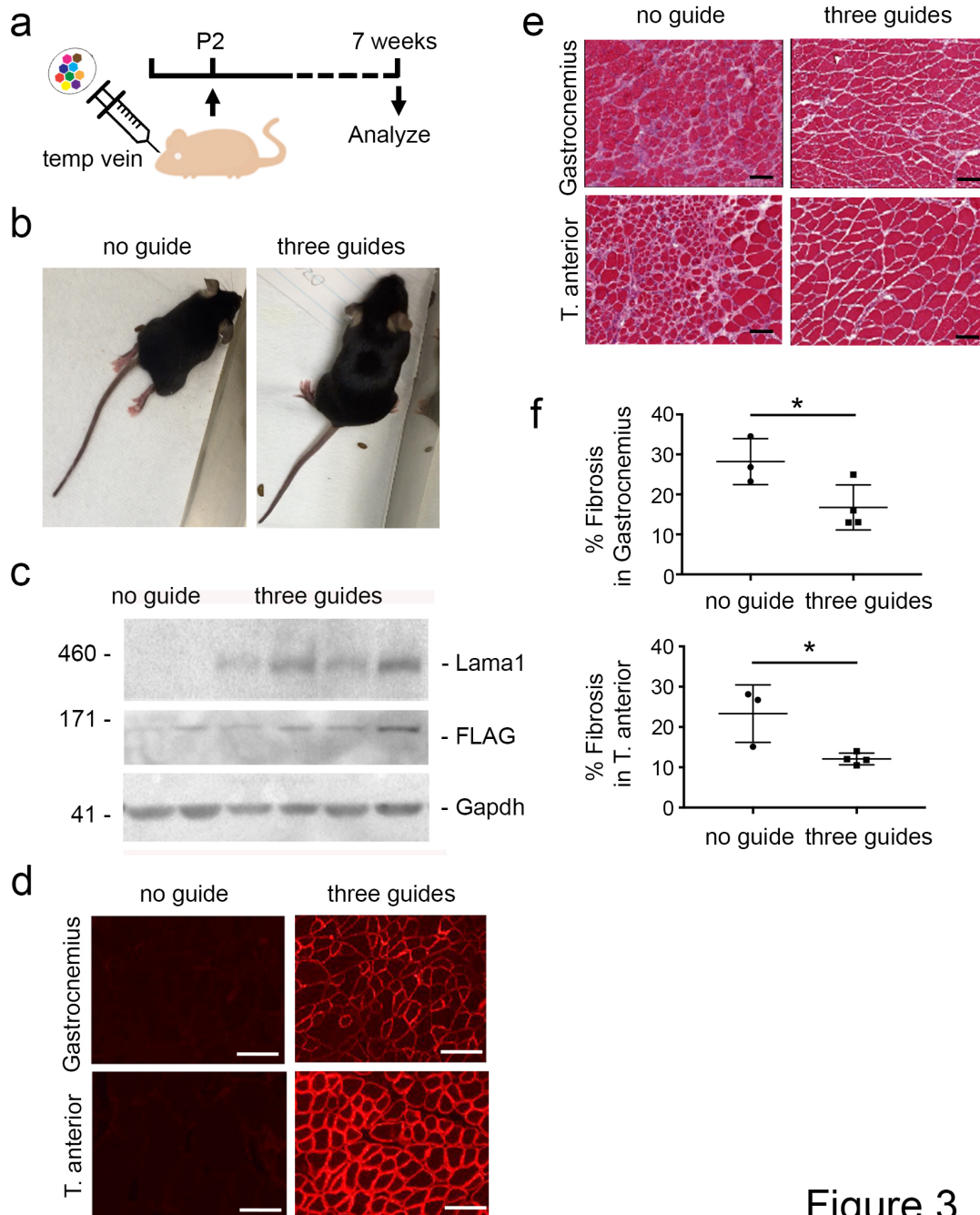


Figure 3

537

538 **Fig. 3. Early intervention to upregulate Lama1 prevents disease progression in**
 539 ***dy^{2j}/dy^{2j}* mice. (a)** Two-day-old neonatal *dy^{2j}/dy^{2j}* mice were injected with AAV9 carrying
 540 no guide (n=3; 7.5x10¹¹ viral genomes) or three guides (n=4; split into two vectors, thus
 541 total dose was 2x7.5x10¹¹ viral genomes) via temporal vein and sacrificed 7 weeks later.
 542 **(b)** Photographs of *dy^{2j}/dy^{2j}* from both treatment groups prior to sacrificing. Note the

543 difference in hindlimb contractures. Lama1 expression was analyzed by (c) western blot
544 and (d) immunofluorescence staining, and general histopathology was evaluated by (e)
545 H&E staining. The muscle groups analyzed are indicated on each panel, except on (c),
546 which shows tibialis anterior (TA) muscles. Scale bars: 100 μm (d), 200 μm (e). (f) The
547 percentage of fibrosis from gastrocnemius (upper) and TA (lower) muscles are
548 calculated and presented as mean \pm standard deviation. Statistical analysis was
549 performed using Student's *t*-test. * $P < 0.05$.

550

551

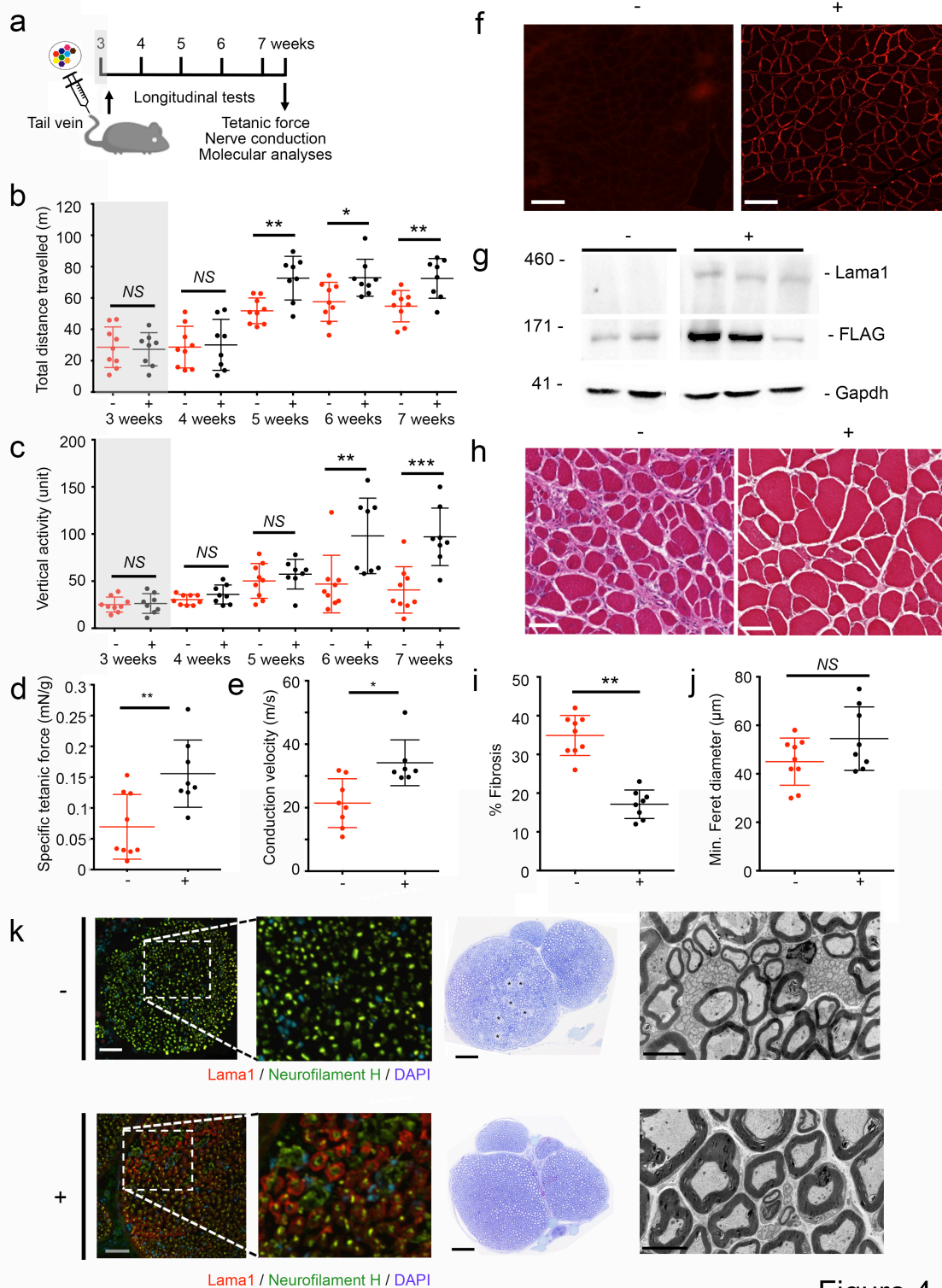


Figure 4

552

553 **Fig. 4. Upregulation of Lama1 in older dy^{2j}/dy^{2j} mice halts disease progression.**

554 (a) Three-week old dy^{2j}/dy^{2j} mice were injected with AAV9 carrying no guide (denoted as
555 -; n=9; 3×10^{11} viral genomes/gram) or three guides (denoted as +; n=6; split into two
556 vectors, thus total dose was $2 \times 3 \times 10^{11}$ viral genomes/gram) via tail vein. Grey box
557 represents period before treatment. (b, c) Open field activity assay was performed
558 weekly, before (grey-shaded) and after treatment, and the mice were tested for (d)
559 muscle contractile and (e) nerve conduction velocity at the end of the treatment regimen,
560 prior to molecular analyses of the tissues. (f) Immunofluorescence staining and (g)
561 western blot to analyze Lama1 expression and (h) H&E staining to quantify (i) fibrosis
562 and (j) fiber size were performed on gastrocnemius muscles. (k) Sciatic nerves were
563 stained for Lama1 (red) and Neurofilament H (green) (left). Nuclei were counterstained
564 by DAPI (blue). Higher magnification images from the dotted area are shown.
565 Representative toluidine blue staining (middle) and electron micrograph (right) are
566 shown. Asterisks indicate region of amyelinated axon fibers. Scale bars: 100 μm (f), 50
567 μm (h), and 200 μm (k). Data are presented as mean \pm standard deviation. Statistical
568 analysis was performed using Student's *t*-test. * $P < 0.05$. ** $P < 0.01$.

569

570

571 References

572

- 573 1. Dowling, J. J., H, D. G., Cohn, R. D., Campbell, C. Treating pediatric neuromuscular
574 disorders: The future is now. *American journal of medical genetics. Part A* 2017.
- 575 2. Gawlik, K., Miyagoe-Suzuki, Y., Ekblom, P., Takeda, S., Durbeej, M. Laminin alpha1
576 chain reduces muscular dystrophy in laminin alpha2 chain deficient mice. *Human*
577 *molecular genetics* 13:16. 2004.
- 578 3. Yurchenco, P. D., McKee, K. K., Reinhard, J. R., Ruegg, M. A. Laminin-deficient
579 muscular dystrophy: Molecular pathogenesis and structural repair strategies. *Matrix*
580 *biology : journal of the International Society for Matrix Biology* 2017.
- 581 4. Kemaladewi, D. U., Maino, E., Hyatt, E., Hou, H., Ding, M., Place, K. M., Zhu, X.,
582 Bassi, P., Baghestani, Z., Deshwar, A. G., Merico, D., Xiong, H. Y., Frey, B. J.,
583 Wilson, M. D., Ivakine, E. A., Cohn, R. D. Correction of a splicing defect in a mouse
584 model of congenital muscular dystrophy type 1A using a homology-directed-repair-
585 independent mechanism. *Nat Medicine*. 23:8. 2017.
- 586 5. Sunada, Y., Bernier, S. M., Utani, A., Yamada, Y., Campbell, K. P. Identification of a
587 novel mutant transcript of laminin alpha 2 chain gene responsible for muscular
588 dystrophy and dysmyelination in dy2J mice. *Human molecular genetics* 4:6. 1995.
- 589 6. Gawlik, K. I., Harandi, V. M., Cheong, R. Y., Petersen, A., Durbeej, M. Laminin alpha1
590 reduces muscular dystrophy in dy(2J) mice. *Matrix biology : journal of the*
591 *International Society for Matrix Biology* 2018.
- 592 7. Gawlik, K. I., Li, J. Y., Petersen, A., Durbeej, M. Laminin alpha1 chain improves
593 laminin alpha2 chain deficient peripheral neuropathy. *Human molecular genetics*
594 15:18. 2006.

- 595 8. Gawlik, K. I., Mayer, U., Blomberg, K., Sonnenberg, A., Ekblom, P., Durbeej, M.
596 Laminin alpha1 chain mediated reduction of laminin alpha2 chain deficient muscular
597 dystrophy involves integrin alpha7beta1 and dystroglycan. *FEBS letters* 580:7. 2006.
- 598 9. Gawlik, K. I., Akerlund, M., Carmignac, V., Elamaa, H., Durbeej, M. Distinct roles for
599 laminin globular domains in laminin alpha1 chain mediated rescue of murine laminin
600 alpha2 chain deficiency. *PloS one* 5:7. 2010.
- 601 10. Gawlik, K. I., Durbeej, M. Transgenic overexpression of laminin alpha1 chain in
602 laminin alpha2 chain-deficient mice rescues the disease throughout the lifespan.
603 *Muscle & nerve* 42:1. 2010.
- 604 11. Maeder, M. L., Linder, S. J., Cascio, V. M., Fu, Y., Ho, Q. H., Joung, J. K. CRISPR
605 RNA-guided activation of endogenous human genes. *Nature methods* 10:10. 2013.
- 606 12. Perez-Pinera, P., Kocak, D. D., Vockley, C. M., Adler, A. F., Kabadi, A. M., Polstein,
607 L. R., Thakore, P. I., Glass, K. A., Ousterout, D. G., Leong, K. W., Guilak, F.,
608 Crawford, G. E., Reddy, T. E., Gersbach, C. A. RNA-guided gene activation by
609 CRISPR-Cas9-based transcription factors. *Nature methods* 10:10. 2013.
- 610 13. Gonzalez, S., Fernando, R. N., Perrin-Tricaud, C., Tricaud, N. In vivo introduction of
611 transgenes into mouse sciatic nerve cells in situ using viral vectors. *Nature protocols*
612 9:5. 2014.
- 613 14. Wojtal, D., Kemaladewi, D. U., Malam, Z., Abdullah, S., Wong, T. W., Hyatt, E.,
614 Baghestani, Z., Pereira, S., Stavropoulos, J., Mouly, V., Mamchaoui, K., Muntoni, F.,
615 Voit, T., Gonorazky, H. D., Dowling, J. J., Wilson, M. D., Mendoza-Londono, R.,
616 Ivakine, E. A., Cohn, R. D. Spell Checking Nature: Versatility of CRISPR/Cas9 for
617 Developing Treatments for Inherited Disorders. *Am J Hum Genet* 98:1. 2016.
- 618 15. Ran, F. A., Cong, L., Yan, W. X., Scott, D. A., Gootenberg, J. S., Kriz, A. J., Zetsche,
619 B., Shalem, O., Wu, X., Makarova, K. S., Koonin, E. V., Sharp, P. A., Zhang, F. In
620 vivo genome editing using *Staphylococcus aureus* Cas9. *Nature* 520:7546. 2015.
- 621 16. Esvelt, K. M., Mali, P., Braff, J. L., Moosburner, M., Yaung, S. J., Church, G. M.
622 Orthogonal Cas9 proteins for RNA-guided gene regulation and editing. *Nature*
623 *methods* 10:11. 2013.
- 624 17. Qi, L. S., Larson, M. H., Gilbert, L. A., Doudna, J. A., Weissman, J. S., Arkin, A. P.,
625 Lim, W. A. Repurposing CRISPR as an RNA-guided platform for sequence-specific
626 control of gene expression. *Cell* 152:5. 2013.
- 627 18. Liao, H. K., Hatanaka, F., Araoka, T., Reddy, P., Wu, M. Z., Sui, Y., Yamauchi, T.,
628 Sakurai, M., O'Keefe, D. D., Nunez-Delgado, E., Guillen, P., Campistol, J. M., Wu, C.
629 J., Lu, L. F., Esteban, C. R., Izpisua Belmonte, J. C. In Vivo Target Gene Activation
630 via CRISPR/Cas9-Mediated Trans-epigenetic Modulation. *Cell* 171:7. 2017.
- 631 19. Pasteuning-Vuhman, S., Putker, K., Tanganyika-de Winter, C. L., Boertje-van der
632 Meulen, J. W., van Vliet, L., Overzier, M., Plomp, J. J., Aartsma-Rus, A., van Putten,
633 M. Natural disease history of the dy2J mouse model of laminin alpha2 (merosin)-
634 deficient congenital muscular dystrophy. *PloS one* 13:5. 2018.
- 635 20. Kemaladewi, D. U., Benjamin, J., Hyatt, E., Ivakine, E. A., Cohn, R. D. Increased
636 polyamine as protective disease modifier in Congenital Muscular Dystrophy. *Human*
637 *molecular genetics* 2018.
- 638 21. Bonnemann, C. G., Wang, C. H., Quijano-Roy, S., Deconinck, N., Bertini, E.,
639 Ferreira, A., Muntoni, F., Sewry, C., Beroud, C., Mathews, K. D., Moore, S. A., Bellini,
640 J., Rutkowski, A., North, K. N., Members of International Standard of Care Committee
641 for Congenital Muscular, D. Diagnostic approach to the congenital muscular
642 dystrophies. *Neuromuscular disorders : NMD* 24:4. 2014.
- 643 22. Qiao, C., Li, J., Zhu, T., Draviam, R., Watkins, S., Ye, X., Chen, C., Li, J., Xiao, X.
644 Amelioration of laminin-alpha2-deficient congenital muscular dystrophy by somatic

- 645 gene transfer of miniagrin. *Proceedings of the National Academy of Sciences of the*
646 *United States of America* 102:34. 2005.
- 647 23. Bentzinger, C. F., Barzaghi, P., Lin, S., Ruegg, M. A. Overexpression of mini-agrin in
648 skeletal muscle increases muscle integrity and regenerative capacity in laminin-
649 alpha2-deficient mice. *FASEB journal : official publication of the Federation of*
650 *American Societies for Experimental Biology* 19:8. 2005.
- 651 24. Qiao, C., Dai, Y., Nikolova, V. D., Jin, Q., Li, J., Xiao, B., Li, J., Moy, S. S., Xiao, X.
652 Amelioration of Muscle and Nerve Pathology in LAMA2 Muscular Dystrophy by AAV9-
653 Mini-Agrin. *Molecular Therapy* 9:2018.
- 654 25. Meinen, S., Barzaghi, P., Lin, S., Lochmuller, H., Ruegg, M. A. Linker molecules
655 between laminins and dystroglycan ameliorate laminin-alpha2-deficient muscular
656 dystrophy at all disease stages. *The Journal of cell biology* 176:7. 2007.
- 657 26. Reinhard, J. R., Lin, S., McKee, K. K., Meinen, S., Crosson, S. C., Sury, M., Hobbs,
658 S., Maier, G., Yurchenco, P. D., Ruegg, M. A. Linker proteins restore basement
659 membrane and correct LAMA2-related muscular dystrophy in mice. *Science*
660 *translational medicine* 9:396. 2017.
- 661 27. McKee, K. K., Crosson, S. C., Meinen, S., Reinhard, J. R., Ruegg, M. A., Yurchenco,
662 P. D. Chimeric protein repair of laminin polymerization ameliorates muscular
663 dystrophy phenotype. *The Journal of clinical investigation* 127:3. 2017.
- 664 28. Hightower, R. M., Alexander, M. S. Genetic modifiers of Duchenne and
665 facioscapulohumeral muscular dystrophies. *Muscle & nerve* 57:1. 2018.
- 666 29. Rooney, J. E., Gurpur, P. B., Burkin, D. J. Laminin-111 protein therapy prevents
667 muscle disease in the mdx mouse model for Duchenne muscular dystrophy.
668 *Proceedings of the National Academy of Sciences of the United States of America*
669 106:19. 2009.
- 670 30. Perrin, A., Rousseau, J., Tremblay, J. P. Increased Expression of Laminin Subunit
671 Alpha 1 Chain by dCas9-VP160. *Molecular therapy. Nucleic acids* 6:2017.
- 672 31. Yuan, J., Ma, Y., Huang, T., Chen, Y., Peng, Y., Li, B., Li, J., Zhang, Y., Song, B.,
673 Sun, X., Ding, Q., Song, Y., Chang, X. Genetic Modulation of RNA Splicing with a
674 CRISPR-Guided Cytidine Deaminase. *Molecular cell* 72:2. 2018.
- 675 32. Villiger, L., Grisch-Chan, H. M., Lindsay, H., Ringnalda, F., Pogliano, C. B., Allegri,
676 G., Fingerhut, R., Haberle, J., Matos, J., Robinson, M. D., Thony, B., Schwank, G.
677 Treatment of a metabolic liver disease by in vivo genome base editing in adult mice.
678 *Nature medicine* 24:10. 2018.
- 679 33. Bengtsson, N. E., Hall, J. K., Odom, G. L., Phelps, M. P., Andrus, C. R., Hawkins, R.
680 D., Hauschka, S. D., Chamberlain, J. R., Chamberlain, J. S. Muscle-specific
681 CRISPR/Cas9 dystrophin gene editing ameliorates pathophysiology in a mouse
682 model for Duchenne muscular dystrophy. *Nature communications* 8:2017.
- 683 34. Nelson, C. E., Hakim, C. H., Ousterout, D. G., Thakore, P. I., Moreb, E. A., Rivera,
684 R. M., Madhavan, S., Pan, X., Ran, F. A., Yan, W. X., Asokan, A., Zhang, F., Duan,
685 D., Gersbach, C. A. In vivo genome editing improves muscle function in a mouse
686 model of Duchenne muscular dystrophy. *Science* 2015.
- 687 35. Tabebordbar, M., Zhu, K., Cheng, J. K., Chew, W. L., Widrick, J. J., Yan, W. X.,
688 Maesner, C., Wu, E. Y., Xiao, R., Ran, F. A., Cong, L., Zhang, F., Vandenberghe, L.
689 H., Church, G. M., Wagers, A. J. In vivo gene editing in dystrophic mouse muscle and
690 muscle stem cells. *Science* 2015.
- 691 36. Long, C., Amoasii, L., Mireault, A. A., McAnally, J. R., Li, H., Sanchez-Ortiz, E.,
692 Bhattacharyya, S., Shelton, J. M., Bassel-Duby, R., Olson, E. N. Postnatal genome
693 editing partially restores dystrophin expression in a mouse model of muscular
694 dystrophy. *Science* 2015.

- 695 37. Thakore, P. I., D'Ippolito, A. M., Song, L., Safi, A., Shivakumar, N. K., Kabadi, A. M.,
696 Reddy, T. E., Crawford, G. E., Gersbach, C. A. Highly specific epigenome editing by
697 CRISPR-Cas9 repressors for silencing of distal regulatory elements. *Nature methods*
698 12:12. 2015.
- 699 38. Lamar, K. M., Bogdanovich, S., Gardner, B. B., Gao, Q. Q., Miller, T., Earley, J. U.,
700 Hadhazy, M., Vo, A. H., Wren, L., Molkentin, J. D., McNally, E. M. Overexpression of
701 Latent TGFbeta Binding Protein 4 in Muscle Ameliorates Muscular Dystrophy through
702 Myostatin and TGFbeta. *PLoS genetics* 12:5. 2016.
- 703 39. Quattrocelli, M., Capote, J., Ohiri, J. C., Warner, J. L., Vo, A. H., Earley, J. U.,
704 Hadhazy, M., Demonbreun, A. R., Spencer, M. J., McNally, E. M. Genetic modifiers of
705 muscular dystrophy act on sarcolemmal resealing and recovery from injury. *PLoS*
706 *genetics* 13:10. 2017.
- 707 40. Kemaladewi, D. U., de Gorter, D. J., Aartsma-Rus, A., van Ommen, G. J., ten Dijke,
708 P., t Hoen, P. A., Hoogaars, W. M. Cell-type specific regulation of myostatin signaling.
709 *FASEB journal : official publication of the Federation of American Societies for*
710 *Experimental Biology* 26:4. 2012.
- 711 41. Zhang, Y., Argaw, A. T., Gurfein, B. T., Zameer, A., Snyder, B. J., Ge, C., Lu, Q. R.,
712 Rowitch, D. H., Raine, C. S., Brosnan, C. F., John, G. R. Notch1 signaling plays a
713 role in regulating precursor differentiation during CNS remyelination. *Proceedings of*
714 *the National Academy of Sciences of the United States of America* 106:45. 2009.
- 715 42. Hakim, C. H., Wasala, N. B., Pan, X., Kodippili, K., Yue, Y., Zhang, K., Yao, G.,
716 Haffner, B., Duan, S. X., Ramos, J., Schneider, J. S., Yang, N. N., Chamberlain, J. S.,
717 Duan, D. A Five-Repeat Micro-Dystrophin Gene Ameliorated Dystrophic Phenotype in
718 the Severe DBA/2J-mdx Model of Duchenne Muscular Dystrophy. *Molecular therapy.*
719 *Methods & clinical development* 6:2017.
- 720 43. Kim, D., Langmead, B., Salzberg, S. L. HISAT: a fast spliced aligner with low
721 memory requirements. *Nature methods* 12:4. 2015.
- 722 44. Anders, S., Pyl, P. T., Huber, W. HTSeq--a Python framework to work with high-
723 throughput sequencing data. *Bioinformatics* 31:2. 2015.
- 724 45. Ritchie, M. E., Phipson, B., Wu, D., Hu, Y., Law, C. W., Shi, W., Smyth, G. K. limma
725 powers differential expression analyses for RNA-sequencing and microarray studies.
726 *Nucleic acids research* 43:7. 2015.
- 727 46. Bae, S., Park, J., Kim, J. S. Cas-OFFinder: a fast and versatile algorithm that
728 searches for potential off-target sites of Cas9 RNA-guided endonucleases.
729 *Bioinformatics* 30:10. 2014.
- 730
731

Extended data/supplementary figures

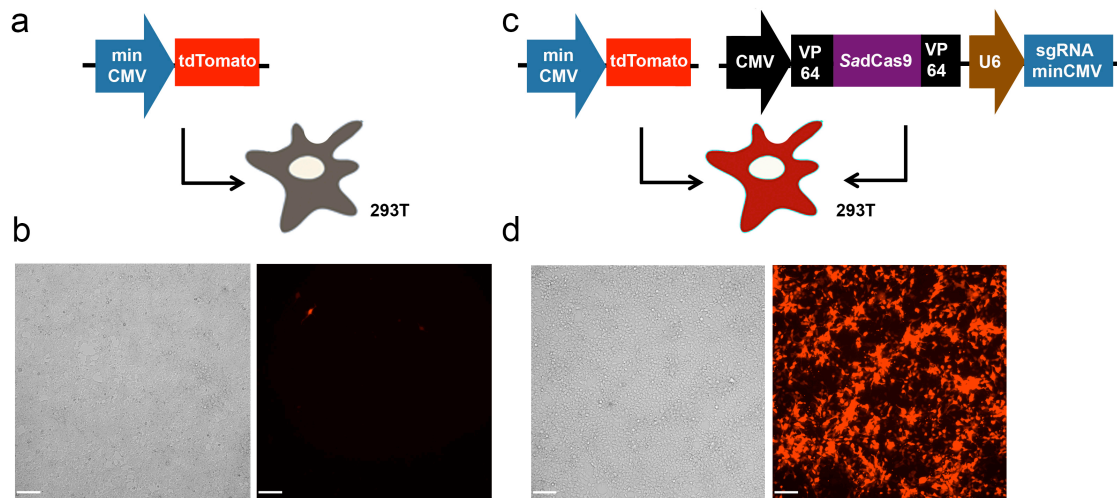


Figure S1

Fig. S1. SadCas9-2xVP64 enhances expression of minCMV-driven *tdTomato* in vitro. HEK293T was transfected with (a,b) a plasmid containing minCMV-driven *tdTomato* gene only, or (c,d) in combination with a plasmid containing SadCas9-2xVP64 and a sgRNA targeting the minCMV promoter. (b,d) Cells were imaged for *tdTomato* expression by fluorescent microscopy. Scale bar: 50 μ m.

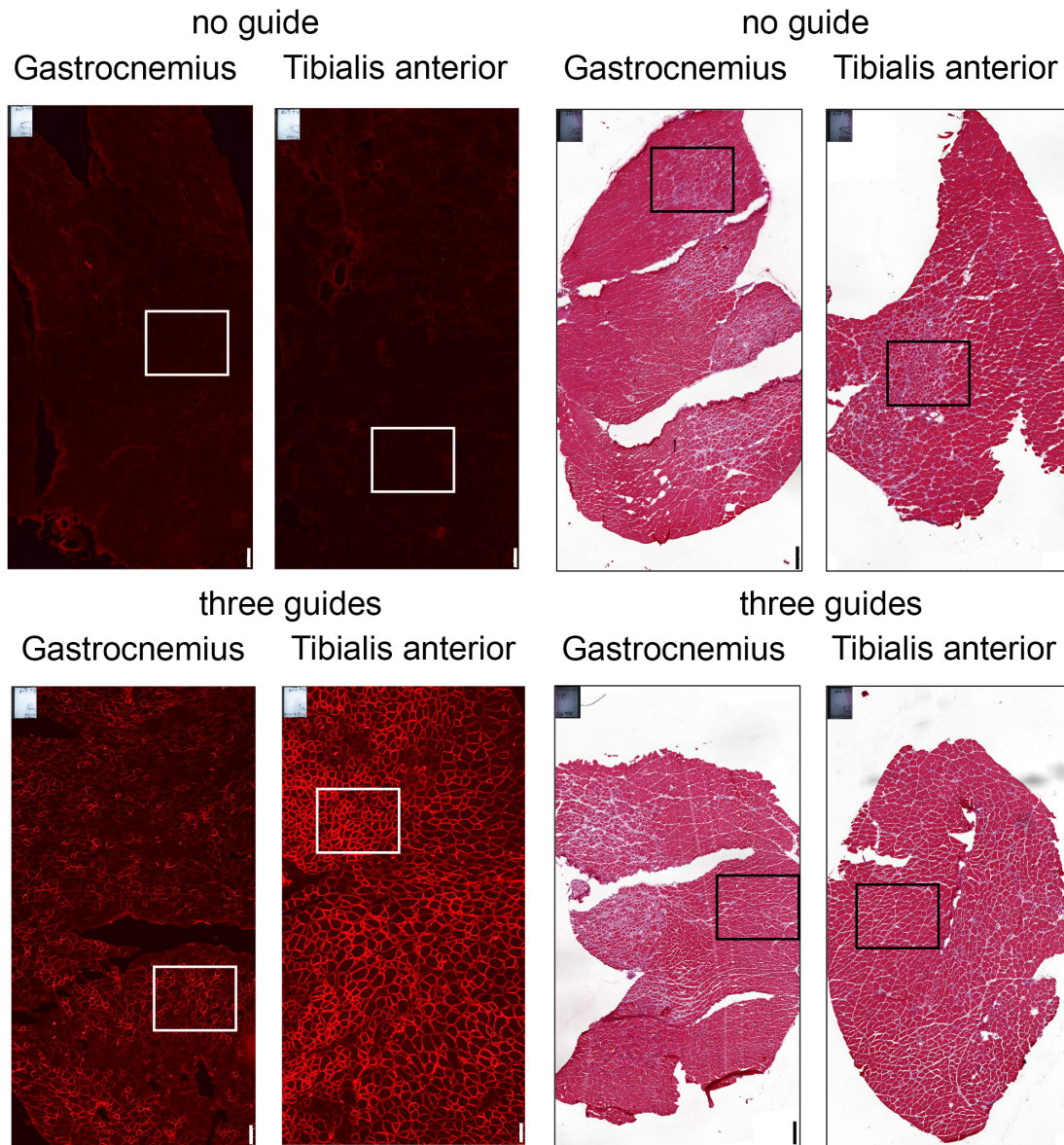


Figure S2

Fig. S2. Expression of Lama1 and muscle architecture following early intervention in neonatal dy^{2j}/dy^{2j} mice. Lower magnification of immunofluorescence and H&E staining images of Fig. 3 in the main manuscript.

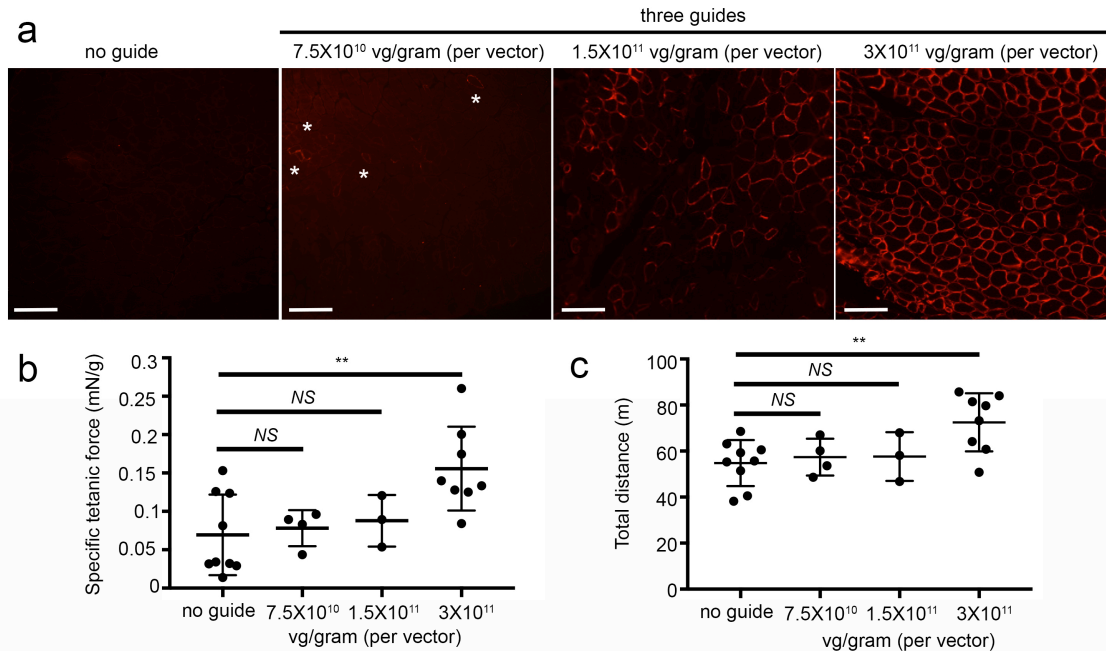


Figure S3

Fig. S3. Upregulation of Lama1 corresponds to improvement of muscle functions.

Three-weeks old dy^{2j}/dy^{2j} mice were injected systemically via tail vein with different doses of AAV9: 7.5×10^{10} , 1.5×10^{11} , or 3×10^{11} viral genome (vg)/gram of mouse. Two AAVs were necessary for the three guide cohort, therefore the total doses of virus injected was 1.5×10^{11} , 3×10^{11} , and 6×10^{11} viral genomes/gram of mouse. TA muscles isolated four weeks later were stained for Lama1 expression (**a**). Asterisks indicate Lama1-positive fibers in the low dose cohort. Scale bar: 100 μ m. *In vivo* contractile force assay (**b**) and open field test (**c**) performed in the end of the treatment regimen. Data are presented as average \pm standard deviation. Statistical analysis was performed using one-way ANOVA. NS: not significant. ** $P < 0.01$.

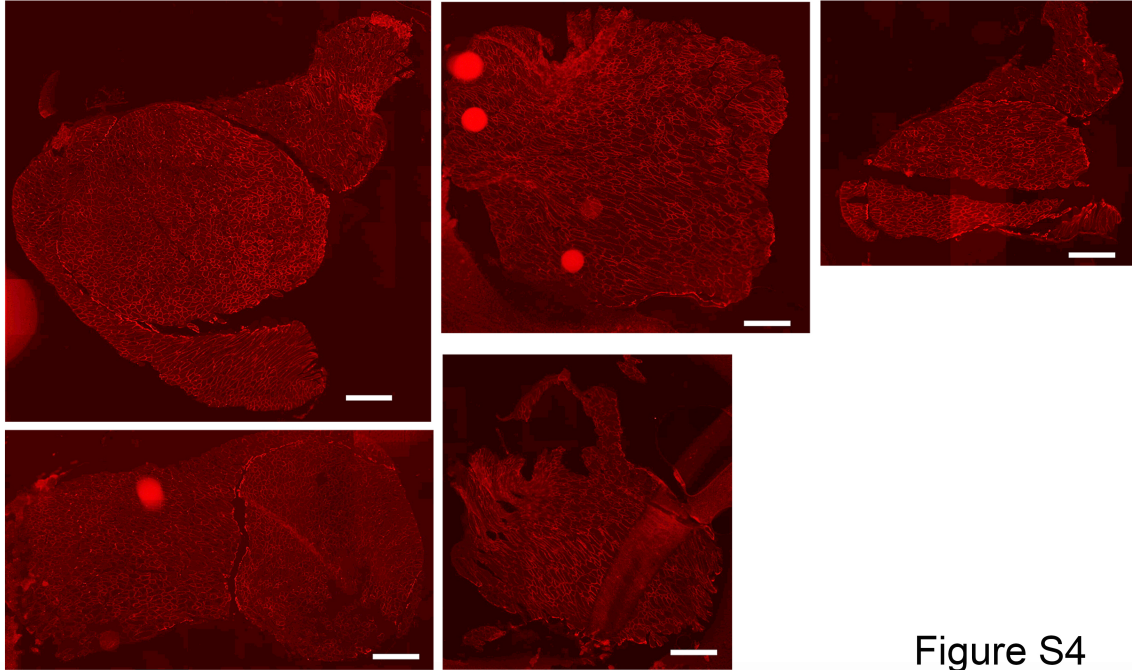


Figure S4

Fig. S4. Representative images of Lama1-positive muscle sections

Mice were injected systemically with three guides at the age of three weeks old via tail vein, and sacrificed at the age of 11-12 weeks old. Muscles were stained for Lama1 expression (red). Scale bar: 500 μ m.

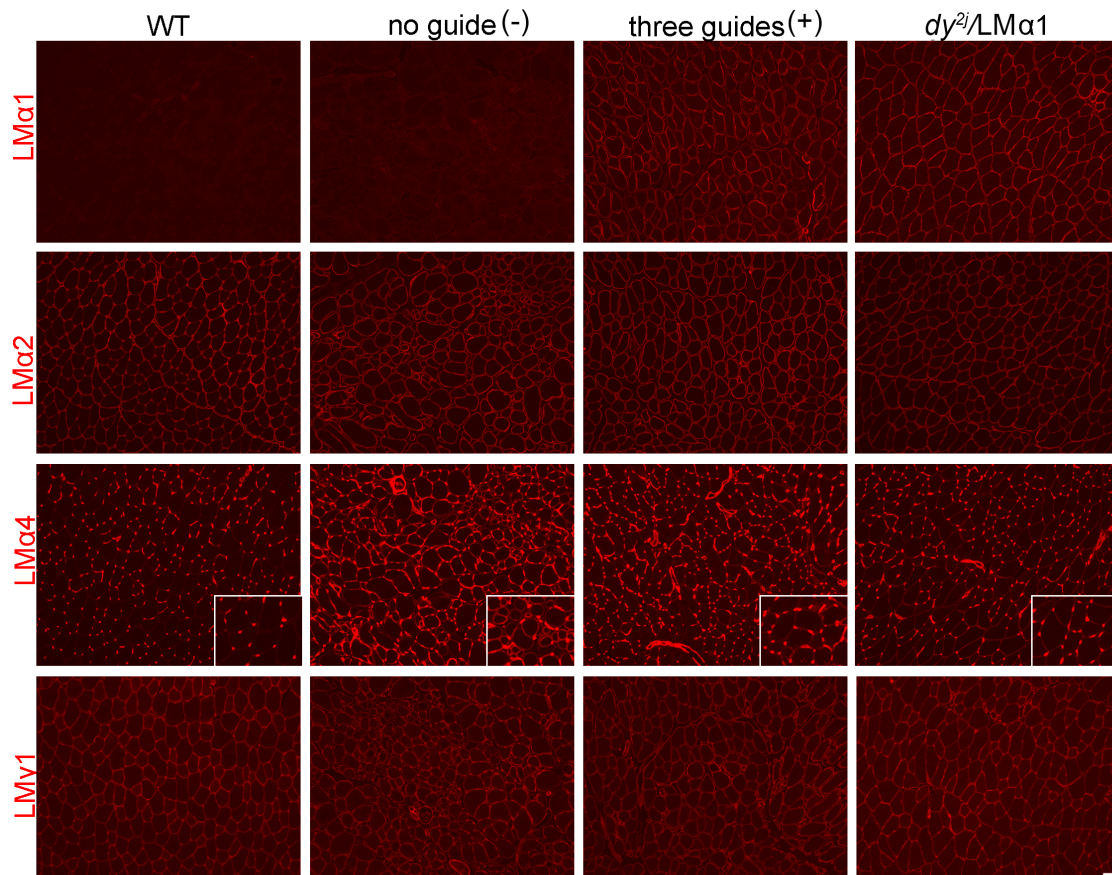


Figure S5

Fig. S5. Expression of Laminin (LM) subunits in tibialis anterior muscles.

Expression of LM subunits in tibialis anterior from wild-type, dy^{2j}/dy^{2j} (intravenously injected with AAV carrying no guide or three guides) and $dy^{2j}/LM\alpha 1$ (with transgenic overexpression of LM $\alpha 1$) mice (n=3 for each group). Expression of LM $\alpha 1$ chain in tibialis anterior is comparable between dy^{2j}/dy^{2j} AAV-three guide-treated mice and transgenic mice. No major differences in expression of LM $\alpha 2$ and LM $\gamma 1$ were detected between the groups. LM $\alpha 4$ chain is upregulated in muscle from dy^{2j}/dy^{2j} AAV-no guide-treated mice and its expression is partially normalized in muscle from dy^{2j}/dy^{2j} AAV-three guide treated mice. Scale bar: 50 μ m.

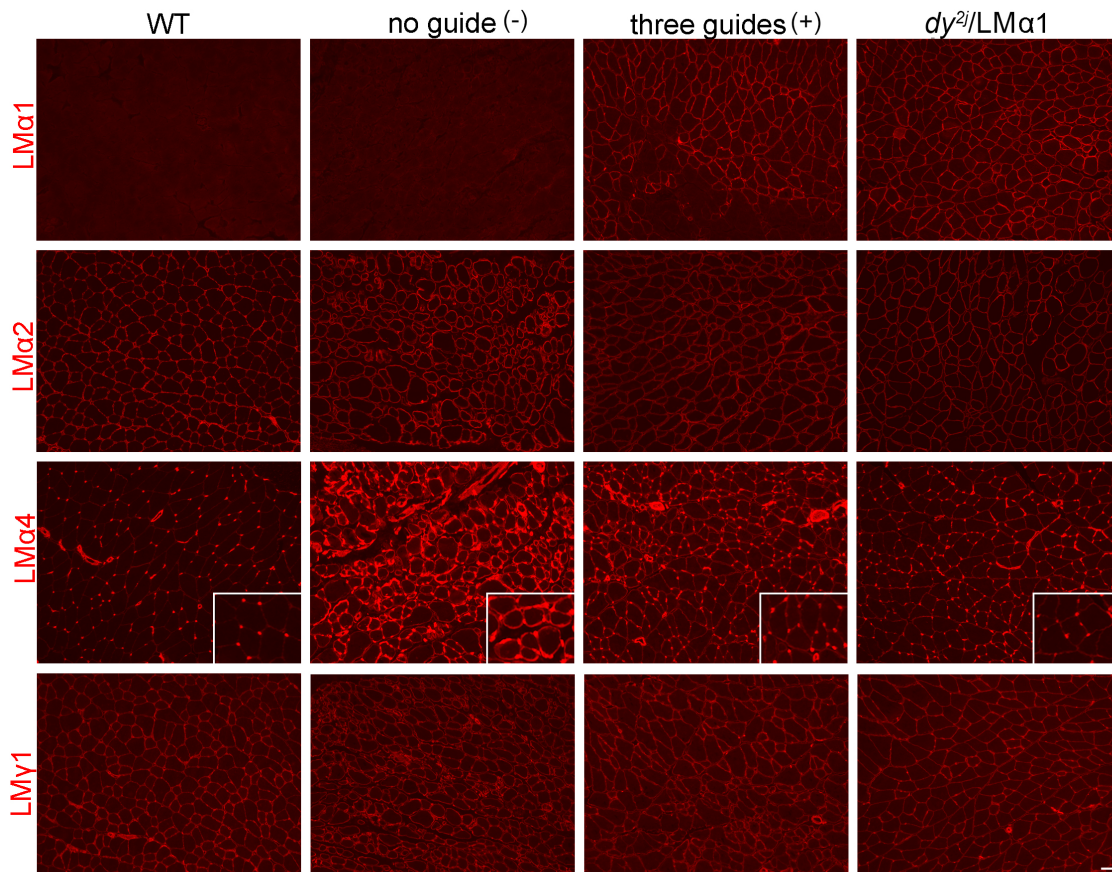


Figure S6

Fig. S6. Expression of Laminin (LM) subunits in gastrocnemius muscles.

Expression of LM subunits in tibialis anterior from wild-type, *dy^{2j}/dy^{2j}* (intravenously injected with AAV carrying no guide or three guides) and *dy^{2j}/LMα1* (with transgenic overexpression of LMα1) mice (n=3 for each group). Expression of LMα1 chain in tibialis anterior is comparable between *dy^{2j}/dy^{2j}* AAV-three guide-treated mice and transgenic mice. No major differences in expression of LMα2 and LMγ1 were detected between the groups. LMα4 chain is upregulated in muscle from *dy^{2j}/dy^{2j}* AAV-no guide-treated mice and its expression is partially normalized in muscle from *dy^{2j}/dy^{2j}* AAV-three guide treated mice. Scale bar: 50μm.

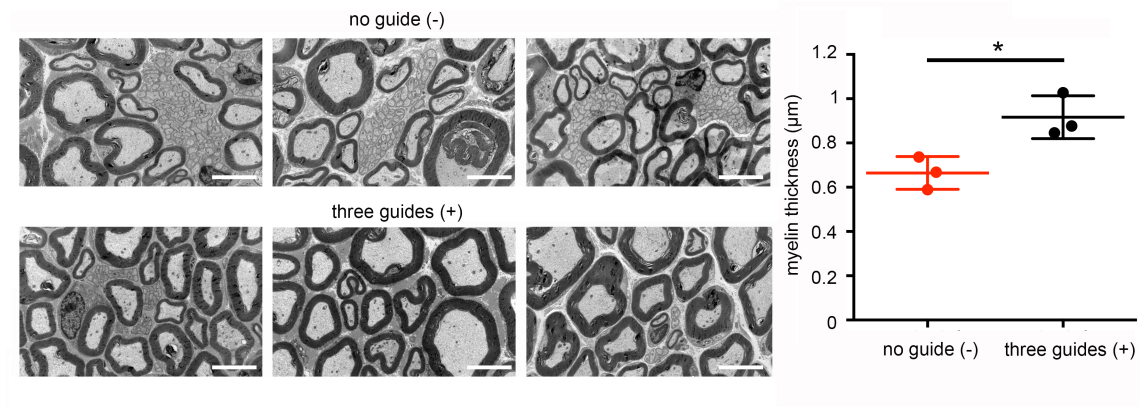


Figure S7

Fig. S7. Myelination of sciatic nerves.

Electron microscopy images of sciatic nerves isolated from dy^{2j}/dy^{2j} mice injected with AAV carrying no guide or three guides (n=3 for each group). Myelin thickness was quantified using ImageJ and presented as average \pm standard deviation. Statistical analysis was performed using Student's *t*-test. * $P < 0.05$. Scale bar: 5 μ m.

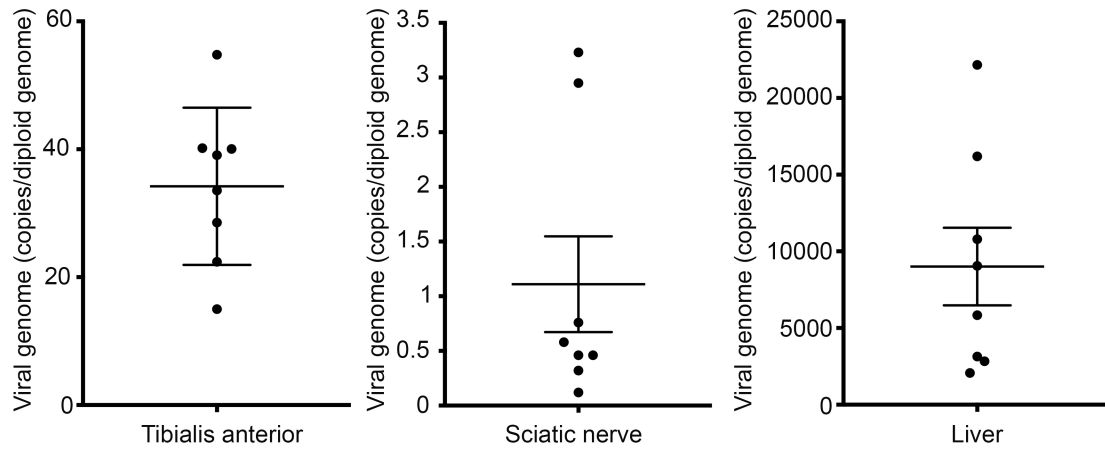


Figure S8

Fig. S8. Quantitative evaluation of AAV genome distribution.

Genomic DNA isolated from tibialis anterior muscle, sciatic nerve and liver of dy2j mice injected with AAV carrying three guides (n=8) was amplified for the presence of viral genome by qPCR. Data are presented as average \pm SEM.

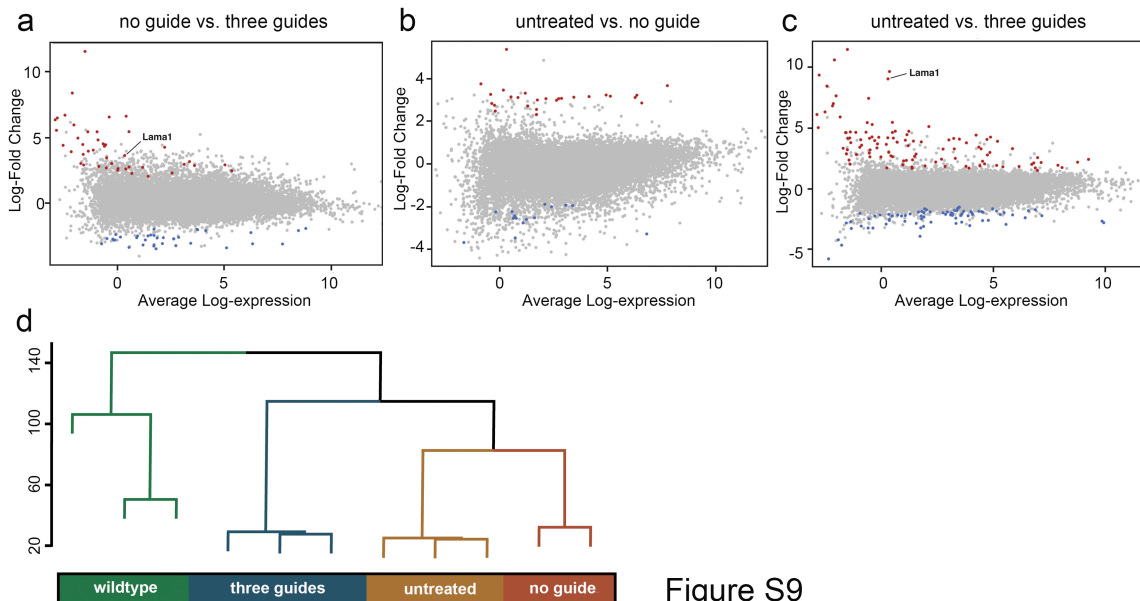


Figure S9

Fig. S9. Genome-wide analysis of gene expression of SadCas9-VP64-treated dy^{2j}/dy^{2j} mice.

Differential expression analysis derived from RNA-Sequencing results from the quadriceps of treated and untreated mice (a-c), comparing SadCas9-2xVP64 alone and SadCas9-2xVP64 with three guides targeting *Lama1* (a), untreated to SadCas9-2xVP64 alone (b), and untreated to SadCas9-2xVP64 with three guides targeting *Lama1* (c). Gene significantly differentially expressed, (FDR < 0.05), are coloured. Red data points indicate a log-fold change greater than one, while blue data points indicate a log-fold change less than one. Hierarchical clustering was performed on the normalized counts-per-million expression data (d).

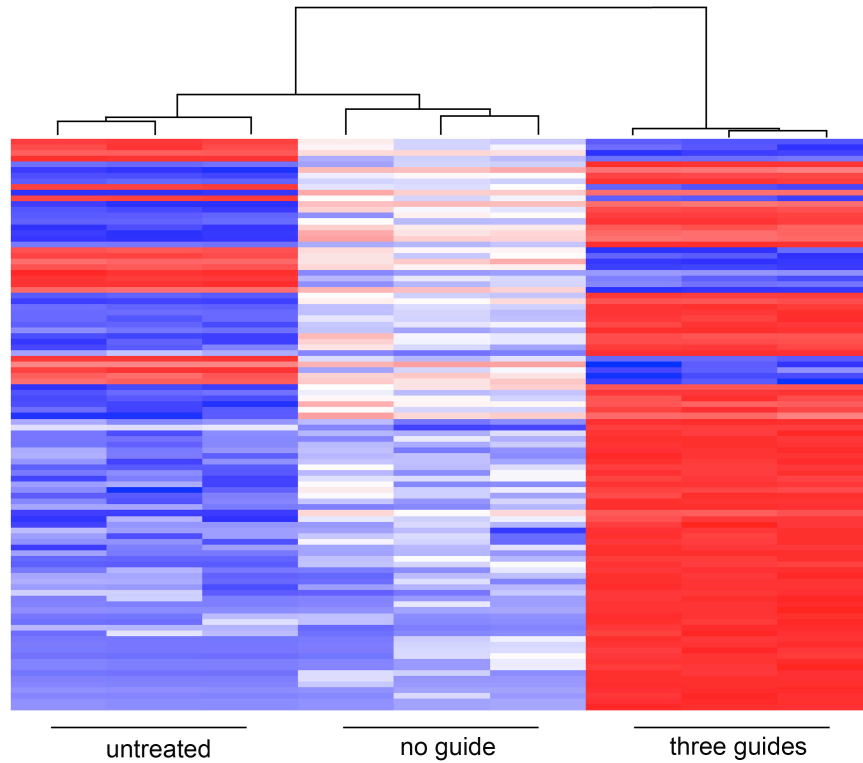


Figure S10

Fig. S10. Top 100 differentially expressed genes.

Heatmap illustrating normalized log-CPM values for the top 100 genes differentially expressed in SadCas9-2xVP64 with three guide treated quadriceps versus untreated quadriceps. Red indicates higher expression while blue indicates lower expression.

Supplemental video legends

Video S1. Phenotype of control dy^{2j}/dy^{2j} mouse following early intervention.

The dy^{2j}/dy^{2j} mouse was injected with AAV9 containing *SadCas9-2xVP64* (no guide) at P2 (pre-symptomatic stage) via temporal vein and video was taken at the age of 7-week old. Hind limb paralysis, contracture and kyphosis resulting from lack of functional *Lama2* and compensatory *Lama1* are apparent.

Video S2. Phenotype of treated dy^{2j}/dy^{2j} mouse following early intervention.

The dy^{2j}/dy^{2j} mouse was injected with AAV9 containing *SadCas9-2xVP64* and sgRNAs targeting *Lama1* proximal promoter (three guides) at P2 (pre-symptomatic stage) via temporal vein and video was taken at the age of 7-week old. Upregulation of compensatory *Lama1* expression ameliorates the hind limb paralysis, contracture and kyphosis.

Video S3. Phenotype of control dy^{2j}/dy^{2j} mouse following intervention at symptomatic stage.

The dy^{2j}/dy^{2j} mouse was injected with AAV9 containing *SadCas9-2xVP64* (no guide) at 3-week old (pre-symptomatic stage) via tail vein. Video was taken at the age of 7-week old. Hind limb paralysis, contracture and kyphosis resulting from lack of functional *Lama2* and compensatory *Lama1* are apparent.

Video S4. Phenotype of treated dy^{2j}/dy^{2j} mouse following intervention at symptomatic stage.

The dy^{2j}/dy^{2j} mouse was injected with AAV9 containing *SadCas9-2xVP64* and sgRNAs targeting *Lama1* proximal promoter (three guides) at 3-week old (pre-symptomatic stage) via tail vein. Video was taken at the age of 7-week old. Dystrophic features and disease progression were significantly improved and partially reversed following upregulation of *Lama1*.

Supplemental tables

Supplemental table 1. Top 100 genes differentially expressed in “SadCas9-2xVP64 + three guides” compared to “untreated”

Supplemental table 2. Top 100 genes differentially expressed in “SadCas9-2xVP64 + three guides” compared to “SadCas9-2xVP64 + no guide”

Supplemental table 3. Top 100 genes differentially expressed in “SadCas9-2xVP64 + no guide” compared to “untreated”

Supplemental table 4. Analysis showing distance from off-target site to differentially expressed gene body

Supplemental table 5. List of computationally predicted off-target sites

Supplemental table 6. Primers, plasmids and sgRNAs used in this study

Supplemental Table 1. Top 100 genes differentially expressed in "SadCas9-2xVP64 + three guides" compared to "untreated"

SYMBOL	TXCHROM	logFC	AveExpr	t	P.Value	adj.P.Val
Ces1c	chr8	8.06720501	-4.0858727	25.0852651	7.60E-11	1.10E-06
1810053823	chr16	10.5369617	-2.0993569	17.6475033	2.81E-09	6.76E-06
Fabp1	chr6	7.92790193	-3.3988185	18.7401814	1.44E-09	6.76E-06
1700003G13	chr9	7.85466761	-3.8132313	17.9773962	2.19E-09	6.76E-06
Cyp2c69	chr19	6.79884139	-4.4022125	17.5155103	2.77E-09	6.76E-06
Slc7a4	chr16	5.42020681	0.54904376	17.737618	2.38E-09	6.76E-06
Ttr	chr18	8.97781797	-3.6645933	17.0207698	3.88E-09	7.51E-06
Apoa2	chr1	5.40091384	-0.6005275	16.7716387	4.16E-09	7.51E-06
Lama1	chr17	8.98321051	0.34708087	15.7290019	8.52E-09	1.37E-05
ApoB	chr12	7.80234986	-3.4299405	15.0813327	1.26E-08	1.82E-05
Tat	chr8	5.3144494	-3.9814489	14.66332	1.58E-08	2.07E-05
Serpina1c	chr12	8.1709174	-3.2361681	14.3754788	2.04E-08	2.27E-05
Fam25c	chr14	7.39071119	-0.5378939	14.4492017	1.90E-08	2.27E-05
Serpina3k	chr12	9.29387622	-2.7989697	13.9984407	2.72E-08	2.81E-05
Igf1	chr11	6.69308056	-4.2970164	13.6072358	3.38E-08	3.26E-05
Mup3	chr4	7.59035385	-2.0248159	13.5095555	3.70E-08	3.35E-05
Rdh7	chr10	6.12757345	-4.306269	12.9783192	5.31E-08	4.07E-05
Gys2	chr6	4.5777154	-1.5679355	13.0234776	5.00E-08	4.07E-05
Wnt4	chr4	4.20831956	5.03311767	12.9293649	5.35E-08	4.07E-05
Gc	chr5	8.24180382	-3.5843802	12.9381073	5.75E-08	4.07E-05
Klrg2	chr6	4.59908759	-1.1223193	12.8010591	5.92E-08	4.07E-05
Srrm4os	chr5	4.04588484	3.61138985	12.4826437	7.52E-08	4.94E-05
Matl1a	chr14	7.36113899	-3.7343781	12.3707009	8.71E-08	5.47E-05
Alb	chr5	9.586285	0.41592462	12.2174291	1.04E-07	6.01E-05
Serpina1a	chr12	6.95305368	-3.6425688	12.1347225	1.04E-07	6.01E-05
Azgp1	chr5	6.86136461	-4.0619138	11.9945852	1.16E-07	6.46E-05
Fgb	chr3	7.48821994	-3.1735567	11.6312338	1.59E-07	8.50E-05
Cidea	chr18	5.07510399	2.21493926	11.4830743	1.71E-07	8.82E-05
9030619P08	chr15	3.92341807	-0.2600478	11.3463138	1.89E-07	9.42E-05
Fgg	chr3	7.33395248	-3.4152783	11.1329778	2.41E-07	0.00011613
Mmd2	chr5	6.67105341	-3.3145461	11.0364562	2.58E-07	0.00012028
Cyp3a11	chr5	8.17360921	-3.6630995	10.8836274	3.06E-07	0.00013811
Slc27a2	chr2	6.6827	-3.1819203	10.7687412	3.26E-07	0.00014295
Ambp	chr4	6.13758126	-3.4506026	10.6633966	3.54E-07	0.00015057
Fga	chr3	7.62720297	-3.9076478	10.5588289	4.03E-07	0.00016636
Samd11	chr4	4.11178696	-0.4979967	10.4245456	4.25E-07	0.00017075
Fabp4	chr3	2.15462805	9.01447477	10.3115148	4.68E-07	0.00018279
Ighg1	chr12	8.46471745	-3.4389537	10.3557091	4.95E-07	0.00018754
Lctf1	chr9	4.2237416	-0.3808795	10.2088981	5.19E-07	0.00018754
Pvalb	chr15	2.52928689	12.8626777	10.2161746	5.11E-07	0.00018754
Apoa5	chr9	6.60004476	-4.1263676	10.219239	5.36E-07	0.00018765
Vps13c	chr9	-2.1668504	3.212495	-10.146085	5.45E-07	0.00018765
Gm4841	chr18	3.86778458	5.35415478	9.78492273	7.72E-07	0.00025932
Prkar2b	chr12	3.97928004	3.13121334	9.7483776	8.00E-07	0.00026274
Pdpr	chr8	-2.203443	3.2904627	-9.4808172	1.03E-06	0.00033107
Hhip1	chr12	-2.7573871	2.31203806	-9.4137394	1.10E-06	0.00034623
Epn3	chr11	4.58955952	-1.5891827	9.3486758	1.19E-06	0.00036635
Aldh1a7	chr19	3.50528717	1.27190747	9.26652168	1.28E-06	0.00038529
Apoa1	chr9	8.39321713	-2.4434213	9.24069066	1.44E-06	0.00042593
Aspg	chr12	4.61360624	-0.6564861	9.09955804	1.53E-06	0.00044273
Adgrd1	chr5	-2.427791	3.44722048	-8.9858424	1.70E-06	0.00048062
Kng1	chr16	5.95942358	-3.7065193	8.99480646	1.75E-06	0.00048561
Ucp1	chr8	11.3963873	-1.5055582	9.07259957	1.85E-06	0.000504
Cps1	chr1	5.87067733	-3.3848414	8.82056311	2.09E-06	0.00055915
Sfrp4	chr13	-3.0424407	4.08490344	-8.7250934	2.23E-06	0.00058511
Jmjd1c	chr10	-3.2313535	1.84643433	-8.5191608	2.77E-06	0.00071562
Orm2	chr4	6.27368915	-2.5305119	8.54126641	2.83E-06	0.00071836
Atp6v1g1	chr4	1.90407218	8.11437097	8.46629447	2.93E-06	0.00072976
NA	NA	3.54327015	-0.8576183	8.37633903	3.24E-06	0.00079375
Elovl6	chr3	3.24419618	3.37792107	8.22580012	3.81E-06	0.0009186
Plg	chr17	4.98742747	-2.84041	8.16368792	4.16E-06	0.00098659
Pzp	chr6	6.39214719	-3.2228911	8.11448596	4.53E-06	0.00105615
Thrsp	chr7	3.26554164	6.03631914	7.85593444	5.77E-06	0.00131835
Gfpt2	chr11	-2.0366124	3.28844052	-7.8437333	5.84E-06	0.00131835
Bhmt	chr13	6.2546489	-3.2262881	7.78687551	6.55E-06	0.00145525
Apoc3	chr9	6.95422106	-2.1511746	7.78192704	6.70E-06	0.00146687
Proca1	chr11	2.63255929	1.56171029	7.68968505	6.97E-06	0.00150381
Hpd	chr5	6.45914605	-3.386459	7.69200292	7.34E-06	0.00156002
Pcsk6	chr7	-1.8922339	4.14311915	-7.6077764	7.67E-06	0.00160525
Dnajb13	chr7	5.86226504	-1.8392095	7.50871687	8.97E-06	0.0018516
NA	NA	-2.8570014	1.63865163	-7.4503139	9.23E-06	0.00187895
Myo5b	chr18	2.30425852	1.18853647	7.43398437	9.40E-06	0.00188746
Fam213b	chr4	2.52777314	7.1852214	7.33239481	1.06E-05	0.00210163
Aldob	chr4	6.06208644	-2.8991635	7.31447554	1.14E-05	0.0021888
Uox	chr3	5.46798424	-3.8910942	7.31419174	1.12E-05	0.0021888
NA	NA	-3.0351581	12.8448432	-7.2578878	1.16E-05	0.00221053
Mrln	chr10	1.89226589	5.31305923	7.19570826	1.25E-05	0.00234855
Me1	chr9	1.9768026	6.91692293	7.13418269	1.35E-05	0.00243628
Agbl1	chr7	-2.0885962	1.3608529	-7.1465611	1.33E-05	0.00243628
NA	NA	-2.9421529	5.7414647	-7.1386369	1.34E-05	0.00243628
NA	NA	-2.8056988	10.2088761	-7.0774684	1.45E-05	0.00258145
Trpm1	chr7	2.96315703	0.3806044	7.01294075	1.57E-05	0.00276221
Cstf6	chr19	2.23495652	4.66958372	7.00007046	1.59E-05	0.00276912
Igtp	chr11	1.86743947	4.54464325	6.89217296	1.82E-05	0.00312869
NA	NA	4.69385795	0.68222882	6.84250559	1.97E-05	0.00331558
Med12	chrX	-2.8614945	3.45721138	-6.8346408	1.96E-05	0.00331558
Serpina1d	chr12	6.32897767	-3.6602287	6.8549536	2.01E-05	0.00334534
NA	NA	4.3761592	4.3735629	6.78718488	2.11E-05	0.00342487
Kcnk3	chr5	3.81800932	1.86995833	6.77998928	2.11E-05	0.00342487
Car5b	chrX	2.17094632	2.52751196	6.69419221	2.34E-05	0.00374934
Aldh1a2	chr9	-3.9155062	1.81350194	-6.6857214	2.38E-05	0.0037799
Grem2	chr1	2.40181819	2.79352205	6.59957294	2.64E-05	0.00414096
Ces1d	chr8	4.10023518	3.35125626	6.59264986	2.69E-05	0.00417708
Ston1	chr17	-2.2562933	0.96729497	-6.573946	2.72E-05	0.00418839
Hpx	chr7	4.63301432	-1.3730015	6.56670755	2.80E-05	0.0042629
ApoH	chr11	2.91855783	-0.5038737	6.52074789	2.92E-05	0.00432487
Ces5a	chr8	2.60133348	0.55171618	6.51934336	2.93E-05	0.00432487
Dpp6	chr5	-2.9196681	0.2619482	-6.5178887	2.93E-05	0.00432487
NA	NA	-3.2449209	-0.3411066	-6.4875991	3.06E-05	0.00445983
Hist1h4i	chr13	1.82127787	3.91078129	6.41227049	3.36E-05	0.00485751

Supplemental Table 2. Top 100 genes differentially expressed in "SadCas9-2xVP64 + three guides" compared to "SadCas9-2xVP64 no guide"

SYMBOL	TXCHROM	logFC	AveExpr	t	P.Value	adj.P.Val
Ces1c	chr8	7.68192528	-4.0858727	23.7177026	1.33E-10	1.92E-06
Tat	chr8	6.51413216	-3.9814489	18.7406265	1.40E-09	1.01E-05
Sic7a4	chr16	5.42395906	0.54904376	16.666776	4.43E-09	1.30E-05
Cyp2c69	chr19	6.41356165	-4.4022125	16.3517656	5.46E-09	1.30E-05
Fabp1	chr6	7.01430136	-3.3988185	16.2688646	5.82E-09	1.30E-05
1810053B23	chr16	8.36567269	-2.0993569	16.2583139	6.04E-09	1.30E-05
Ttr	chr18	8.59253823	-3.6645933	16.1987709	6.30E-09	1.30E-05
Apoa2	chr1	4.31309488	-0.6005275	13.99838	2.46E-08	4.44E-05
1700003G13	chr9	6.16709101	-3.8132313	13.5514729	3.48E-08	5.59E-05
Rdh7	chr10	6.27061455	-4.306269	13.3403682	4.07E-08	5.88E-05
Apob	chr12	6.36042846	-3.4299405	11.8844821	1.26E-07	0.00015264
Alb	chr5	6.60124813	0.41592462	11.8383922	1.31E-07	0.00015264
Gc	chr5	7.61086889	-3.5843802	11.8108876	1.37E-07	0.00015264
Mup3	chr4	5.93703811	-2.0248159	11.5983687	1.58E-07	0.00016265
Igf1bp1	chr11	5.77947999	-4.2970164	11.4236063	1.82E-07	0.00017145
Serpina1a	chr12	6.56777394	-3.6425688	11.3493672	1.97E-07	0.00017145
Fam25c	chr14	4.42384018	-0.5378939	11.2759968	2.02E-07	0.00017145
Klrg2	chr6	4.01555522	-1.1223193	11.016482	2.51E-07	0.000195
Serpina1c	chr12	6.4833408	-3.2361681	10.992408	2.67E-07	0.000195
Fgg	chr3	7.23133838	-3.4152783	10.9526164	2.81E-07	0.000195
Fgb	chr3	7.10294021	-3.1735567	10.9405546	2.83E-07	0.000195
Kif1a	chr1	-3.2035885	1.72216362	-10.578571	3.68E-07	0.0002416
Lama1	chr17	3.60580481	0.34708087	10.3369068	4.59E-07	0.00028082
Serpina3k	chr12	6.46825197	-2.7989697	10.3674744	4.66E-07	0.00028082
Kng1	chr16	6.59377507	-3.7065193	10.145317	5.74E-07	0.00033198
Fga	chr3	7.24192323	-3.9076478	9.94497979	7.04E-07	0.00039142
Cidea	chr18	4.23425211	2.21493926	9.56079601	9.62E-07	0.00050767
Mat1a	chr14	5.91921759	-3.7343781	9.56655238	9.84E-07	0.00050767
Cyp3a11	chr5	7.26000864	-3.6630995	9.49753456	1.09E-06	0.00054116
Cadm4	chr7	-3.0854364	3.43404374	-9.3112336	1.22E-06	0.00058834
Sic27a2	chr2	5.77735647	-3.1819203	9.16142955	1.47E-06	0.00068446
Ucp1	chr8	11.5394284	-1.5055582	9.19742703	1.63E-06	0.00073752
Myo5b	chr18	2.70815964	1.18853647	8.91782918	1.82E-06	0.00079698
Mbp	chr18	-3.1241971	6.32564126	-8.796965	2.07E-06	0.00087745
Uox	chr3	6.38500137	-3.8910942	8.81536963	2.13E-06	0.00087745
NA	NA	7.30546168	-3.4389537	8.74748808	2.33E-06	0.00093426
Prx	chr7	-3.432919	5.10990804	-8.6589476	2.39E-06	0.00093426
Mpz	chr1	-3.1391767	7.72442679	-8.5709125	2.62E-06	0.00095901
Samd11	chr4	3.4319878	-0.4979967	8.53270285	2.74E-06	0.00095901
Apoa5	chr9	5.68644419	-4.1263676	8.55205544	2.76E-06	0.00095901
Azgp1	chr5	5.17378801	-4.0619138	8.54116051	2.77E-06	0.00095901
Ambp	chr4	5.00265745	-3.4506026	8.53232871	2.79E-06	0.00095901
Aspg	chr12	4.49864426	-0.6564861	8.45164468	3.02E-06	0.00101368
9030619P08	chr15	2.99612235	-0.2600478	8.36658783	3.27E-06	0.00105887
Sbsn	chr7	-2.6633714	0.90905622	-8.3572564	3.30E-06	0.00105887
Plg	chr17	5.52507799	-2.84041	8.36109263	3.39E-06	0.00106392
Cldn19	chr4	-3.2653338	2.7388015	-8.2964238	3.53E-06	0.00108534
Gys2	chr6	2.88423499	-1.5679355	8.17357339	4.04E-06	0.00121478
Ahsg	chr16	5.41354129	-0.9425466	8.11597943	4.43E-06	0.00130544
Wnt4	chr4	2.89310387	5.03311767	8.06192403	4.57E-06	0.00132035
Srrm4os	chr5	2.83746235	3.61138985	8.01069135	4.84E-06	0.00137073
Apoa1	chr9	6.68102512	-2.4434213	7.80253925	6.50E-06	0.0018055
Elovl6	chr3	3.14304008	3.37792107	7.70931392	6.83E-06	0.00186108
G6pc	chr11	5.60315183	-3.3951407	7.70806009	7.06E-06	0.00187982
Cps1	chr1	5.23974239	-3.3848414	7.6779702	7.26E-06	0.00187982
Aldob	chr4	6.32598423	-2.8991635	7.69579537	7.29E-06	0.00187982
Arg1	chr10	4.44362967	-1.6097834	7.59014941	7.93E-06	0.00201138
Epn3	chr11	3.69453485	-1.5891827	7.53325568	8.41E-06	0.00209514
Hba-a1	NA	-2.2700334	6.2456611	-7.4965888	8.73E-06	0.00213896
Ddn	chr15	-3.398565	0.55130958	-7.2073462	1.24E-05	0.00298201
Fa2h	chr8	-3.2130863	1.20608522	-7.032031	1.53E-05	0.00363058
Cadm3	chr1	-2.051734	3.75756436	-6.9210036	1.75E-05	0.00403033
Ppp1r3b	chr8	2.57692007	0.40173032	6.92011989	1.76E-05	0.00403033
Pzp	chr6	5.50500956	-3.2228911	6.84788224	1.99E-05	0.00449761
Nfasc	chr1	-2.6849138	1.86436923	-6.7931454	2.06E-05	0.00458172
Orm2	chr4	4.38077136	-2.5305119	6.70807897	2.33E-05	0.00506111
Sox10	chr15	-3.2987824	1.71005186	-6.6733195	2.41E-05	0.00506111
Hpx	chr7	5.41271902	-1.3730015	6.697118	2.41E-05	0.00506111
Prkar2b	chr12	2.93206413	3.13121334	6.65445212	2.46E-05	0.00506111
Bmp7	chr2	-2.8365493	-0.1703501	-6.65022	2.47E-05	0.00506111
Ces5a	chr8	2.72830868	0.55171618	6.64349268	2.49E-05	0.00506111
Serpina1d	chr12	6.18935314	-3.6602287	6.67534697	2.52E-05	0.00506111
Dnajb13	chr7	4.93453349	-1.8392095	6.49479192	3.09E-05	0.00612482
Serpinc1	chr1	3.93724606	-1.3533652	6.28356394	4.02E-05	0.0078515
Dact2	chr17	-2.5238997	0.9490797	-6.1621573	4.69E-05	0.00902999
NA	NA	2.77363083	-0.8576183	6.1509308	4.76E-05	0.0090517
Hpd	chr5	5.36870724	-3.386459	6.15556143	4.90E-05	0.0091922
Acsm3	chr7	4.79325628	-0.8979803	6.08513137	5.32E-05	0.00985906
Dusp15	chr2	-2.832713	1.31355423	-5.9744195	6.05E-05	0.0110674
Mag	chr7	-2.4835744	1.72185278	-5.8808295	6.88E-05	0.01242024
2310008N11	chr8	2.47762951	0.0223978	5.78103716	7.90E-05	0.0140903
Aph1c	chr9	2.02542717	1.4446743	5.69597944	8.90E-05	0.01567068
Alas2	chrX	-2.7381939	2.63862482	-5.6882468	9.00E-05	0.01567068
Aldh1a2	chr9	-3.5045852	1.81350194	-5.619936	9.96E-05	0.01713352
Rasgef1c	chr11	-2.7268056	-0.4788461	-5.5831253	0.00010446	0.01760109
Sic9b2	chr3	2.60867469	0.03741035	5.58003047	0.00010488	0.01760109
Sptbn5	NA	-3.1073231	2.1100215	-5.5741903	0.00010597	0.01760109
Aph1	chr11	2.6612831	-0.5038737	5.5623464	0.00010758	0.01766438
Plip	chr8	-2.6544819	2.15418714	-5.5538324	0.00010889	0.01767908
Mgat3	chr15	-2.522372	1.43835928	-5.538076	0.00011133	0.01787536
Spn	chr4	-2.0266173	3.73200949	-5.4989035	0.0001177	0.01857554
Mup11	chr4	6.5359933	-0.3747465	5.54577617	0.00011827	0.01857554
Hbb-bt	NA	-2.1214318	4.13274184	-5.4147076	0.00013289	0.02043237
Kif19a	chr11	-2.4525954	1.56428869	-5.414812	0.00013292	0.02043237
Hepacam	chr9	-3.1235403	-0.7331738	-5.3921781	0.00013769	0.02094399
9130230L23	chr5	2.99937564	-1.7029617	5.3379434	0.00014889	0.0224111
Apoc3	chr9	3.89375921	-2.1511746	5.21346237	0.00018033	0.02686402
Scube1	chr15	-2.61022	0.15037746	-5.1910997	0.00018445	0.02719675
Gal3st1	chr11	-2.7637327	-0.2060749	-5.1771827	0.00018838	0.02749575
Gim4841	chr18	2.44516047	5.35415478	5.13981561	0.00019895	0.02874825

Supplemental Table 3. Top 100 genes differentially expressed in SadCas9-2xVP64-no guide compared to "untreated"

SYMBOL	TXCHROM	logFC	AveExpr	t	P.Value	adj.P.Val
Hba-a1	NA	3.12223892	6.2456611	12.331034	8.43E-08	0.00121768
Mpz	chr1	3.67608141	7.72442679	10.6882893	3.34E-07	0.00241497
Hbb-bt	NA	3.16484723	4.13274184	9.89369815	6.93E-07	0.00244925
Hba-a2	chr11	3.23794544	4.91567042	9.85619618	7.18E-07	0.00244925
Cadm4	chr7	3.13536782	3.43404374	9.68323067	8.47E-07	0.00244925
Mbp	chr18	3.22961817	6.32564126	9.26281665	1.28E-06	0.00308948
Lama1	chr17	5.3774057	0.34708087	8.31143772	3.57E-06	0.0073592
Hbb-bs	chr7	2.8634898	6.55027296	8.1395833	4.19E-06	0.00756795
Prx	chr7	3.18266127	5.10990804	7.96374203	5.11E-06	0.00765789
Cldn19	chr4	3.06808525	2.7388015	7.89212771	5.53E-06	0.00765789
Tlr13	chrX	-2.5987846	1.26055872	-7.8376704	5.88E-06	0.00765789
1700001O22Rik	chr2	3.76078395	-0.8282985	7.77422963	6.36E-06	0.00765789
Ccl2	chr11	-2.7593297	1.1058906	-7.6753655	7.09E-06	0.00788188
Mx1	chr16	-3.4609353	0.74527914	-7.5588781	8.15E-06	0.00804522
Fa2h	chr8	3.32272314	1.20608522	7.53694641	8.35E-06	0.00804522
CSar1	chr7	-1.8891035	2.10571941	-7.258534	1.16E-05	0.01013989
Klf1a	chr1	2.32436318	1.72216362	7.23538702	1.19E-05	0.01013989
Fam178b	chr1	3.0042875	1.76045364	7.10719561	1.40E-05	0.01120779
Ddn	chr15	3.14993822	0.55130958	6.92964353	1.74E-05	0.01322915
Lct1	chr9	3.26770545	-0.3808795	6.88735709	1.83E-05	0.01325713
Plip	chr8	3.06580561	2.15418714	6.82876119	1.97E-05	0.01357527
Lrrc15	chr16	-2.4883765	0.74755506	-6.7582519	2.15E-05	0.01414289
NA	NA	-1.9501553	3.38202652	-6.6526	2.46E-05	0.01547083
Alas2	chrX	2.9899336	2.63862482	6.51840873	2.93E-05	0.01765268
Xist	chrX	-3.2767212	6.77693285	-6.4385364	3.26E-05	0.01864379
Ncmmap	chr4	3.08130356	2.86901463	6.39750506	3.43E-05	0.01864379
Gjb1	chrX	3.46954089	0.2018106	6.38853084	3.48E-05	0.01864379
Mag	chr7	2.56287891	1.72185278	6.3342043	3.73E-05	0.01922711
Snca	chr6	3.12063457	0.87022355	6.30932249	3.86E-05	0.01922711
Ilrl1	chr1	-2.5405179	0.79307145	-6.2535459	4.15E-05	0.01968275
Pvalb	chr15	1.9371664	12.8626777	6.2397791	4.22E-05	0.01968275
Dusp15	chr2	2.72326203	1.31355423	5.89258602	6.77E-05	0.02962619
Adam12	chr7	-2.0037212	2.41708454	-5.8606882	7.07E-05	0.02962619
Ccl7	chr11	-2.540678	0.66322051	-5.838118	7.30E-05	0.02962619
Cd300lb	chr11	-2.4326089	0.71920982	-5.8322784	7.35E-05	0.02962619
Bmp7	chr2	2.48796642	-0.1703501	5.82971426	7.38E-05	0.02962619
Arg1	chr10	-3.6796601	-1.6097834	-5.8042644	7.70E-05	0.03006634
Sfrp1	chr8	-1.9250563	3.06171827	-5.6945804	8.91E-05	0.03389067
Aoah	chr13	-2.230976	0.59804822	-5.5991203	0.00010202	0.0377995
Msr1	chr8	-2.5214491	1.6301269	-5.5421659	0.00011069	0.03942958
Cmtm5	chr14	2.84161366	-0.3319268	5.5243583	0.00011364	0.03942958
Clec4d	chr6	-2.2426926	-0.1450714	-5.5175924	0.0001146	0.03942958
Mmd2	chr5	4.10127424	-3.3145461	5.35972024	0.00014594	0.04854376
Gal3st1	chr11	2.75795131	-0.2060749	5.34218678	0.00014781	0.04854376
Sbspon	chr1	2.22808049	0.44090614	5.22117943	0.00017632	0.05546403
Adams6	chr13	-2.4536128	1.59657982	-5.2204485	0.00017656	0.05546403
Hhip1	chr12	-1.9118394	2.31203806	-5.2007135	0.00018171	0.05586471
Hepacam	chr9	2.91504751	-0.7331738	5.16779439	0.00019114	0.0574251
Fzr1	chr13	-2.2231625	1.71289475	-5.1068931	0.00020888	0.06109392
Gm42067	NA	1.85312529	2.04012111	5.09877039	0.0002114	0.06109392
Adcy7	chr8	-1.881753	4.6834493	-5.0461447	0.00022871	0.06480185
Klf19a	chr11	2.27988907	1.56428869	5.02136549	0.00023743	0.06597873
Tlr8	chrX	-4.0365645	-1.2570211	-4.9449509	0.00027029	0.07369187
Smox	chr2	1.81483923	5.4987099	4.89994085	0.00028521	0.07513181
C3ar1	chr6	-3.095913	2.52727176	-4.897357	0.00028728	0.07513181
Eps8l1	chr7	-2.4924048	2.20261789	-4.8867435	0.00029117	0.07513181
Adgre1	chr17	-1.5575189	3.45468859	-4.8714084	0.00029787	0.07551336
Sfrp4	chr13	-2.0811203	0.08490344	-4.8359387	0.00031448	0.07742878
Sfrn4	chr11	-2.7773743	-1.1861611	-4.8334332	0.00031615	0.07742878
Lilr4b	chr10	-3.0117057	2.19904976	-4.7560936	0.00035649	0.08523435
NA	NA	2.2188592	1.46909467	4.74477333	0.00036179	0.08523435
Dupd1	chr14	1.83532553	6.3387283	4.73767715	0.00036571	0.08523435
Cdh1	chr8	2.69435584	0.15753197	4.7105409	0.00038186	0.08758428
Ctbp100	chr6	2.68467385	-0.1085207	4.65308887	0.00041746	0.09425372
Chil3	chr3	-4.4041995	-0.8908455	-4.6368929	0.00043783	0.09733231
NA	NA	-2.032801	1.63865163	-4.5516428	0.00048859	0.10697147
Ms4a7	chr19	-2.0914278	2.7993614	-4.4397996	0.0005829	0.12571458
Pmp22	chr11	1.97966029	7.02265612	4.41974373	0.00060171	0.12720169
Sox10	chr15	2.30301682	1.71005186	4.41400578	0.0006074	0.12720169
Tnc	chr4	-2.1869894	6.29769631	-4.323846	0.00070125	0.14475757
Dclre1c	chr2	-1.798468	1.83339495	-4.2666147	0.00076856	0.15522687
Ccl6	chr11	-1.8144934	4.30576424	-4.2626793	0.00077345	0.15522687
A930016O22Rik	chr7	1.77831878	7.34616069	4.2491595	0.00079047	0.15646948
Spire2	chr8	2.46586051	-0.8626346	4.23290116	0.00081207	0.15857376
Pdpr	chr8	-1.5137564	3.29044627	-4.2177999	0.00083148	0.1601984
Ms4a4a	chr19	-3.3012903	2.04305875	-4.2086143	0.0008496	0.16153672
Retnla	chr16	1.70702394	3.83252031	4.18081523	0.00088276	0.16566021
Igfb6	chr7	-2.1161057	1.14725297	-4.1698631	0.00089871	0.16649164
Bmper	chr9	-2.3781522	3.01926601	-4.1196582	0.00097551	0.17808689
Kcnmb4	chr10	2.06573485	-0.0707184	4.1071686	0.00099511	0.17808689
Cenpi	chrX	-3.2736233	-0.9010077	-4.1092747	0.00099827	0.17808689
Tfec	chr6	-2.4975075	-0.9890424	-4.0905242	0.00102332	0.18032955
Ccr1	chr9	-3.5459938	0.74382016	-4.0436169	0.00111601	0.19199831
Serpine1	chr5	-1.6929341	4.20045863	-4.0366477	0.00111654	0.19199831
G530011O06Rik	chrX	-3.0056326	0.28110767	-4.0255271	0.00114176	0.19199831
Ptger2	chr14	-2.2297542	-0.7377989	-4.0227253	0.00114269	0.19199831
Lilrb4a	chr10	-4.0994493	0.16994375	-3.9912293	0.00123047	0.20437115
Rnf180	chr13	-1.9538557	-0.0378799	-3.9618891	0.00126259	0.20522254
Ccl12	chr11	-2.0439673	-0.1216011	-3.9612473	0.001264	0.20522254
Mjmd1c	chr10	-1.8859772	1.84643433	-3.942432	0.00130374	0.20875585
Myh4	chr11	1.82246949	13.9035537	3.93272021	0.00132479	0.20875585
Cd33	chr7	-2.5021255	1.96787566	-3.931379	0.0013291	0.20875585
Fam25c	chr14	2.96687101	-0.5378939	3.90989754	0.00138126	0.21461452
Ccr5	chr9	-3.1584851	1.7062355	-3.9018754	0.0014026	0.21561211
Sostdc1	chr12	2.54871926	-0.5067107	3.88711315	0.00143042	0.21757481
Ccnb1	chr13	-2.1828154	0.91827463	-3.8617101	0.0014905	0.22309683
Nuf2	chr1	-2.3761242	0.99193462	-3.8590906	0.00149761	0.22309683
Fgf16	chrX	-2.4858276	0.08167528	-3.850861	0.00151877	0.22347127
Naip6	chr13	-3.0919726	-0.73325	-3.8332285	0.00157101	0.22347127

Supplemental Table 4. Analysis showing distance from off-target site to differentially expressed gene body

SYMBOL	TXCHROM	logFC	adj.P.Val	Gene start (bp)	Gene end (bp)	Off-Target Sequence	Chromosome	Site (bp)	to Gene (bp)	matches	Strand	Lama1 Guide
Ces1c	chr8	8.06720501	1.10E-06	93099015	93131283	aggggGCaGgGCaGcCaGcAGGCGCTGAGT	chr8	90241651	2857364	9	+	CACCGGGGGCGGGCCAGGCGAGCCNNNNN
Slc7a4	chr16	5.4202681	6.76E-06	17572018	17583214	tgCaAAGAGTctTctGcCCAGGCAAGAAAT	chr16	8237459	9343559	8	+	CACCGAACCACTGGAGTGGAGGNNNNN
Fabp1	chr6	7.92790193	6.76E-06	71199827	71205023	CagCtGcagCtGcTcGcCAGGCTGGAAT	chr6	72989175	1784152	8	+	CACCGAAGGGCTGGCAGCAGCCNNNNN
1700003G13R1k	chr9	7.85466761	6.76E-06	45318265	45322079	ataCaAaacGcTcaGctGcCAGGCTAGAT	chr9	43733430	1584835	9	+	CACCGAAGGGCTGGCAGCAGCCNNNNN
Cyp2e9	chr19	6.79884139	6.76E-06	39842660	39867679	gAcGgCaGagCctGcTtGcCAGGCGGGGT	chr19	40318577	431808	9	+	CACCGGGGGCGGGCCAGGCGAGCCNNNNN
1810053B23R1k	chr16	10.536917	6.76E-06	93342504	93366668	CACtGAtGAtCctTcGcCAGGCTGGAT	chr16	93058037	284467	9	+	CACCGAAGGGCTGGCAGCAGCCNNNNN
Apoa2	chr1	5.40091384	7.51E-06	171225054	171226379	tgGCaCGGGGCaGcGgCaGcAGGCTAGAT	chr1	171081055	143999	9	+	CACCGGGGGCGGGCCAGGCGAGCCNNNNN
Trp1	chr8	8.97781797	7.51E-06	20665250	20674324	AtgtGCaGcagGCaGgCAGGCAAGAAAT	chr8	24331496	3657172	9	+	CACCGGGGGCGGGCCAGGCGAGCCNNNNN
Lama1	chr17	8.98321051	1.37E-05	67697265	67822645	N/A	N/A	N/A	N/A	N/A	N/A	N/A
ApoB	chr12	7.80234966	1.82E-05	7977648	8016835	CAGggGCGcagGCaGgCAGGCGAGGCTGGGT	chr12	8858102	841177	9	+	CACCGGGGGCGGGCCAGGCGAGCCNNNNN
Fat	chr8	5.3144494	2.07E-05	109990437	109999803	aAcCtTtGgCtCtCtCtCAGGCTGAGT	chr8	110878472	878669	9	+	CACCGAAGGGCTGGCAGCAGCCNNNNN
Fam25c	chr14	7.39071119	2.27E-05	34351881	34355433	aACtGACCCAGtgGctGctGcCAGGCTGGAGT	chr14	32562154	1789727	8	+	CACCGAACCAACTGGAGTGGAGGNNNNN
Serpina1c	chr12	8.1709174	2.27E-05	103894926	103904887	ttCacActtGAtTtGGAAGgGAGGCTGGGGT	chr12	105870943	1960656	9	+	CACCGAACCAACTGGAGTGGAGGNNNNN
Serpina3k	chr12	9.29387622	2.81E-05	104338486	104364144	ttCacActtGAtTtGGAAGgGAGGCTGGGGT	chr12	105870943	1524799	9	+	CACCGAACCAACTGGAGTGGAGGNNNNN
Igf1bp1	chr11	6.69380856	3.26E-05	17197782	7202546	tttttAAGGgGtGgGcCtGcCAGGCTGGAT	chr11	7421018	218472	9	+	CACCGAAGGGCTGGCAGCAGCCNNNNN
Mup3	chr4	7.59035385	3.35E-05	62083476	62087342	CAGAaAGGGTgtaactCCAGGCTGGAGT	chr4	63232225	1144883	9	+	CACCGAAGGGCTGGCAGCAGCCNNNNN
Gnt2	chr6	4.5777154	4.07E-05	142422613	142473109	CAGgtATGtTtGtCAGCAGGCTGGAGT	chr6	143140787	667678	9	+	CACCGAAGGGCTGGCAGCAGCCNNNNN
Wys4	chr4	4.20831956	4.07E-05	137277489	137299726	tcCCtTggGcCgCaGcCtCAGGCTGGAT	chr4	137673872	374146	9	+	CACCGAAGGGCTGGCAGCAGCCNNNNN
Rdh7	chr10	6.12757345	4.07E-05	127884028	127888817	ccCGCAAcagCtCaGcCAGGCTGGAGT	chr10	128913811	1024994	9	+	CACCGAAGGGCTGGCAGCAGCCNNNNN
Gc	chr5	8.24180382	4.07E-05	89417522	89457828	CAGgttTGGcggGcCaGcCAGGCTGGAT	chr5	101591226	12133328	9	+	CACCGAAGGGCTGGCAGCAGCCNNNNN
Klrf2	chr6	4.59908759	4.07E-05	38625693	38637242	CggggTctGtGcGgGcCAGGCGAGGCTGGGT	chr6	38551799	73894	9	+	CACCGGGGGCGGGCCAGGCGAGCCNNNNN
Srrm4os	chr5	4.04588484	4.94E-05	116438720	116465487	CcCaGActCtGtTGGAGgGAGGCTGAGAT	chr5	116290065	148655	8	+	CACCGAACCAACTGGAGTGGAGGNNNNN
Mat1a	chr14	7.36113899	5.47E-05	41105035	41124412	gACCaCGGGCtGtGcCAGGCGAGGCTGGAT	chr14	41192606	68194	7	+	CACCGGGGGCGGGCCAGGCGAGCCNNNNN
Alb	chr5	9.586285	6.01E-05	90460897	90476602	CAGgttTGGcggGcCaGcCAGGCTGGAT	chr5	101591226	11114624	9	+	CACCGAAGGGCTGGCAGCAGCCNNNNN
Serpina1a	chr12	6.95305368	6.01E-05	103853589	103863562	ttCacActtGAtTtGGAAGgGAGGCTGGGGT	chr12	105870943	2007381	9	+	CACCGAACCAACTGGAGTGGAGGNNNNN
Azgp1	chr5	6.86136461	6.46E-05	137981520	137990233	CAGtAAGGCTCrtGgCAGGCGAGGCTAGAT	chr5	139375397	1385164	8	+	CACCGAACCAACTGGAGTGGAGGNNNNN
Fgb	chr3	7.48821994	8.50E-05	83040141	83049863	CACcagctGagCtCaCtCtCAGGCTAGAT	chr3	87805463	4755600	9	+	CACCGAAGGGCTGGCAGCAGCCNNNNN
Cidea	chr18	5.07510399	8.82E-05	67343564	67367794	ACtCaAAGGCTgGgTgGtGAGGCTGGGGT	chr18	69341102	1973308	8	+	CACCGAACCAACTGGAGTGGAGGNNNNN
9030619P08R1k	chr15	9.32341807	9.42E-05	75427606	75431829	aAcTtGAtGgCaGcGtCtCAGGCGAGGAT	chr15	76107757	675928	8	+	CACCGAAGGGCTGGCAGCAGCCNNNNN
Fgg	chr12	7.33395248	0.0011613	83007724	83015049	CACcagctGagCtCaCtCtCAGGCTAGAT	chr12	87805463	4790414	9	+	CACCGAAGGGCTGGCAGCAGCCNNNNN
Mmd2	chr5	6.17610541	0.0012028	14626358	146280800	ctttGAGGGGgagGgaaCaCAGGCTGGGT	chr5	142010113	552245	9	+	CACCGAAGGGCTGGCAGCAGCCNNNNN
Cyp3a11	chr5	6.67360921	0.0013811	145854426	145879964	aggCGTGGgagTgCaGcCAGGCTAGAT	chr5	145646342	208084	9	+	CACCGGGGGCGGGCCAGGCGAGCCNNNNN
Slc27a2	chr2	6.6827	0.0014295	126552407	126588243	cttCCACtCtCaGgGgGAGGCTGGGGT	chr2	126819405	231162	9	+	CACCGAACCAACTGGAGTGGAGGNNNNN
Ambp	chr4	6.13758126	0.0015057	61343275	61354799	CAGAaAAGGGCTgtaactCCAGGCTGGAT	chr4	63232225	77426	9	+	CACCGAAGGGCTGGCAGCAGCCNNNNN
Fga	chr3	7.62720297	0.0016636	83026076	83033627	CACcagctGagCtCaCtCtCAGGCTAGAT	chr3	87805463	4771836	9	+	CACCGAAGGGCTGGCAGCAGCCNNNNN
Samd11	chr4	4.11178696	0.0017075	15624696	156255657	CACaGActTgGgaaCaGcCAGGCGAGGAT	chr4	15503906	743060	9	+	CACCGGGGGCGGGCCAGGCGAGCCNNNNN
Fabp4	chr3	2.15462805	0.0018279	10204088	10208576	cttGCaAAGcCaGtGcCAGGCTGAGT	chr3	10144068	60020	9	+	CACCGAAGGGCTGGCAGCAGCCNNNNN
Pvalb	chr15	2.52928689	0.0018754	78191114	78206400	cttCtAActTtGtTGGAGgGAGGCTGGGAT	chr15	78664606	458206	9	+	CACCGAACCAACTGGAGTGGAGGNNNNN
Lct1	chr9	4.2237416	0.0018754	64131747	64138118	aAcTtGAtGgCtCtCtCAGGCTGGAT	chr9	64028355	88792	9	+	CACCGAAGGGCTGGCAGCAGCCNNNNN
NA	NA	8.46471745	0.0018754	113325240	113330523	CgCtAAGtGAtGtCaGcCAGGCTAGAT	chr12	118302511	4927228	8	+	CACCGAAGGGCTGGCAGCAGCCNNNNN
Apoa5	chr9	6.60004476	0.0018765	46268633	46271919	aAcAaAGGCGCTGgGaaCAGGCGAGGAT	chr9	46913410	61491	6	+	CACCGAAGGGCTGGCAGCAGCCNNNNN
Yps13c	chr2	2.1668504	0.0018765	67840396	67895638	aAcCtGAGGCGcAcTtCtCAGGCTGGAT	chr9	69433414	143776	8	+	CACCGAAGGGCTGGCAGCAGCCNNNNN
Kmg48l1	chr18	3.86778458	0.0025932	60268301	60273267	tAtCGtAaAGcTtGtCtCAGGCTAGAT	chr18	61821232	1547965	9	+	CACCGAAGGGCTGGCAGCAGCCNNNNN
Pkr2b	chr12	3.97928004	0.0026274	31958476	32061296	aCtTtGgGcagGgCaGcCAGGCGAGGAT	chr12	30913970	1044506	9	+	CACCGGGGGCGGGCCAGGCGAGCCNNNNN
Pdpr	chr8	-2.203443	0.0033107	111094630	111137074	aAcCtTtGgCtCtCtCAGGCTAGAT	chr8	110878472	216159	9	+	CACCGAAGGGCTGGCAGCAGCCNNNNN
Hhip1	chr12	-2.7573871	0.0034623	108306270	108330869	tgacCtGgGtGtCaGcCAGGCGAGGAT	chr12	106527437	1778833	9	+	CACCGGGGGCGGGCCAGGCGAGCCNNNNN
Epn3	chr11	4.58955952	0.0036635	94489599	94499974	CACaCaCaCaCaGtGAGgGAGGCTGGGT	chr11	9563937	1063963	9	+	CACCGAACCAACTGGAGTGGAGGNNNNN
Aldh1a7	chr9	3.50528717	0.0038529	20692953	20727562	attCAGAGGCTcctGtCtCAGGCTAGAT	chr9	17118070	3574883	9	+	CACCGAAGGGCTGGCAGCAGCCNNNNN
Apoa1	chr9	8.39321713	0.0042593	46228580	46230646	aAcAaAGGCGCTGgGaaCAGGCGAGGAT	chr9	46913410	682944	6	+	CACCGAAGGGCTGGCAGCAGCCNNNNN
Aspp	chr12	4.61360624	0.0044273	112106679	112127559	cttCtGAGGtGtCaGcCAGGCGAGGAT	chr12	106527437	5579242	9	+	CACCGGGGGCGGGCCAGGCGAGCCNNNNN
Adgr1	chr5	-2.427791	0.0048062	129096750	129204599	CAGCaAGtGcCaGtCtCAGGCTGGGT	chr5	128632023	464727	9	+	CACCGAAGGGCTGGCAGCAGCCNNNNN
Kng1	chr16	5.95942358	0.0048561	23057865	23082078	gAGtAGtGtGtGgGtGgGtCAGGCTGGAT	chr16	29714613	6632535	9	+	CACCGAACCAACTGGAGTGGAGGNNNNN
Ucp1	chr8	11.3963873	0.005004	83290352	83298455	tggtGAtCCCAcTtCaATGtGAGGCTAAGAT	chr8	80336949	2954083	8	+	CACCGAACCAACTGGAGTGGAGGNNNNN
Cps1	chr1	5.87067723	0.0055915	61712026	61723125	CAtgTgGgGtGgGtCtCtCAGGCTGGGT	chr1	74579710	7348451	9	+	CACCGGGGGCGGGCCAGGCGAGCCNNNNN
Sfrp4	chr13	-3.042407	0.0058511	19623104	19632994	gAcaAAGtGtCtTgTgCAGGCTAGAT	chr13	20914228	1281234	9	+	CACCGAAGGGCTGGCAGCAGCCNNNNN
Jmjd1c	chr10	-3.2313535	0.0071562	67096125	67256326	tggaacGtGtGtCtCtCAGGCTGGAT	chr10	70037110	2780784	9	+	CACCGGGGGCGGGCCAGGCGAGCCNNNNN
Orm2	chr4	6.27368915	0.0071836	63362449	63365876	CAGAaAAGGGCTgtaactCCAGGCTAGAT	chr4	63232225	130224	9	+	CACCGAAGGGCTGGCAGCAGCCNNNNN
Atp6v1g1	chr4	1.90407218	0.0072976	63544772	63550750	CAGAaAAGGGCTgtaactCCAGGCTAGAT	chr4	63232225	312547	9	+	CACCGAAGGGCTGGCAGCAGCCNNNNN
NA	NA	3.54327015	0.0079375	21753529	21800773	CAtgtGtGGGgagCtGatGtCAGGCGAGAAAT	chr3	19951663	1801866	9	+	CACCGGGGGCGGGCCAGGCGAGCCNNNNN
Elovl6	chr17	3.24418618	0.009186	129532355	129638493	CtCtGtTtGcGcGgGgGgCAGGCTGGAT	chr17	130060165	421820	9	+	CACCGGGGGCGGGCCAGGCGAGCCNNNNN
Pig	chr13	4.98742747	0.0098659	12378609	12419384	CtCtCagAAGcaaaTgGCaACAGGCAAGAT	chr13	11877092	501517	9	+	CACCGAACCAACTGGAGTGGAGGNNNNN
Fp2	chr6	6.39214719	0.0105615	128483567	128526720	gACaaaGGGtGtGcGtGgCAGGCTGGGT	chr6	122781164	5702403	8	+	CACCGGGGGCGGGCCAGGCGAGCCNNNNN
Prr1	chr11	-2.0366124	0.0113135	49794178	49838613	gAtCtTgGtTtGtGtGtCAGGCTAGAT	chr11	48433528	1350650	9	+	CACCGAAGGGCTGGCAGCAGCCNNNNN
Thrsp	chr3	3.26554164	0.0113135	97412938	97417730	CtCtAGtGgGcCaGcCAGGCGAGGCTGGGT	chr7	98123842	706112	9	+	CACCGGGGGCGGGCCAGGCGAGCCNNNNN
Bhmt	chr17	2.5246489	0.0145525	93616675	93637961	ccCtCAcaGtGgaGCaCAGCAGGCGAGAT	chr13	93292572	291791	9	+	CACCGAAGGGCTGGCAGCAGCCNNNNN
ApoC3	chr9	6.95422106	0.0146687	46232933	46235636	aAcAaAAGGCGCTGgGaaCAGGCGAGGAT	chr9	46913410	677774	6	+	CACCGAAGGGCTGGCAGCAGCCNNNNN
Proca1	chr11	2.63255929	0.0150381	78193392	78205763	tgtaaaAaGcCaTgGCaCAGGCGAGGAT	chr11	80531260	2325497	9	+	CACCGAACCAACTGGAGTGGAGGNNNNN
Hsp6	chr5	6.45914605	0.0156002	123171807	123182727	tcCCAGGtGtTtGtTtCAGGCGATGAT	chr5	120699033	2427274	9		

Supplemental Table 5. List of computationally predicted off-target sites

Number	3'aa1 Guide	Chromosome	Off-Target Loc	Off-Target Sequence	Strand	Mismatches
1	CACCGCCCAACTGAGTGAAGGTTNNNN	chr1	1631214	CcAagCTcghTgAGTGTGGAGGTTGGAAAT	-	9
2	CACCGCCCAACTGAGTGAAGGTTNNNN	chr1	2151252	CACAGGaaTcTcTCCACAGGCTCGAGT	-	9
3	CACCGAGGCTCCGCGCAGCGNNNN	chr1	3862493	CtAcAAGGCTcGgTcACAGGAGTGGT	-	9
4	CACCGAGGCTCCGCGCAGCGNNNN	chr1	5141884	CtAcAGGaaCTcTcTCCACAGGAGT	-	9
5	CACCGAGGCTCCGCGCAGCGNNNN	chr1	5058127	CtAcAGGaaCTcTcTCCACAGGAGT	-	9
6	CACCGAGGCTCCGCGCAGCGNNNN	chr1	5726302	gggCAAGGCTCTCCACAGGCGAGT	-	8
7	CACCGAGGCTCCGCGCAGCGNNNN	chr1	5791493	CtAgTcAGGaaTcTcTCCACAGGAGT	-	8
8	CACCGAGGCTCCGCGCAGCGNNNN	chr1	5791618	CtAgTcAGGaaTcTcTCCACAGGAGT	-	8
9	CACCGAGGCTCCGCGCAGCGNNNN	chr1	5791626	CtAgTcAGGaaTcTcTCCACAGGAGT	-	8
10	CACCGAGGCTCCGCGCAGCGNNNN	chr1	7457910	CtAgTcAGGaaTcTcTCCACAGGAGT	-	9
11	CACCGAGGCTCCGCGCAGCGNNNN	chr1	8782223	hACaAGGaaTcTcTCCACAGGAGT	-	8
12	CACCGAGGCTCCGCGCAGCGNNNN	chr1	8786182	hACaAGGaaTcTcTCCACAGGAGT	-	8
13	CACCGAGGCTCCGCGCAGCGNNNN	chr1	9031346	hACaAGGaaTcTcTCCACAGGAGT	-	9
14	CACCGAGGCTCCGCGCAGCGNNNN	chr1	9199513	hACaAGGaaTcTcTCCACAGGAGT	-	9
15	CACCGAGGCTCCGCGCAGCGNNNN	chr1	9235566	CtAgTcAGGaaTcTcTCCACAGGAGT	-	9
16	CACCGCCCAACTGAGTGAAGGTTNNNN	chr1	10964154	gggCAAGGCTCTCCACAGGAGT	-	9
17	CACCGCCCAACTGAGTGAAGGTTNNNN	chr1	12648448	CtAgTcAGGaaTcTcTCCACAGGAGT	-	9
18	CACCGAGGCTCCGCGCAGCGNNNN	chr1	13427663	CtAgTcAGGaaTcTcTCCACAGGAGT	-	9
19	CACCGAGGCTCCGCGCAGCGNNNN	chr1	13501972	hACaAGGaaTcTcTCCACAGGAGT	-	9
20	CACCGCCCAACTGAGTGAAGGTTNNNN	chr1	14115427	CtAgTcAGGaaTcTcTCCACAGGAGT	-	8
21	CACCGAGGCTCCGCGCAGCGNNNN	chr1	15071793	hACaAGGaaTcTcTCCACAGGAGT	-	9
22	CACCGCCCAACTGAGTGAAGGTTNNNN	chr1	15731498	hACaAGGaaTcTcTCCACAGGAGT	-	9
23	CACCGAGGCTCCGCGCAGCGNNNN	chr1	15960336	CtAgTcAGGaaTcTcTCCACAGGAGT	-	9
24	CACCGAGGCTCCGCGCAGCGNNNN	chr1	16190133	CtAgTcAGGaaTcTcTCCACAGGAGT	-	9
25	CACCGAGGCTCCGCGCAGCGNNNN	chr1	16192075	hACaAGGaaTcTcTCCACAGGAGT	-	9
26	CACCGAGGCTCCGCGCAGCGNNNN	chr1	171065806	gggCAAGGCTCTCCACAGGAGT	-	9
27	CACCGAGGCTCCGCGCAGCGNNNN	chr1	171073441	gggCAAGGCTCTCCACAGGAGT	-	9
28	CACCGAGGCTCCGCGCAGCGNNNN	chr1	171081075	gggCAAGGCTCTCCACAGGAGT	-	9
29	CACCGCCCAACTGAGTGAAGGTTNNNN	chr1	17961916	gggCAAGGCTCTCCACAGGAGT	-	9
30	CACCGAGGCTCCGCGCAGCGNNNN	chr1	179800672	hACaAGGaaTcTcTCCACAGGAGT	-	8
31	CACCGAGGCTCCGCGCAGCGNNNN	chr1	180373924	CtAgTcAGGaaTcTcTCCACAGGAGT	-	9
32	CACCGAGGCTCCGCGCAGCGNNNN	chr1	180487362	CtAgTcAGGaaTcTcTCCACAGGAGT	-	9
33	CACCGAGGCTCCGCGCAGCGNNNN	chr1	181119156	hACaAGGaaTcTcTCCACAGGAGT	-	9
34	CACCGAGGCTCCGCGCAGCGNNNN	chr1	182612878	hACaAGGaaTcTcTCCACAGGAGT	-	9
35	CACCGAGGCTCCGCGCAGCGNNNN	chr1	182861831	CtAgTcAGGaaTcTcTCCACAGGAGT	-	9
36	CACCGAGGCTCCGCGCAGCGNNNN	chr1	18543466	hACaAGGaaTcTcTCCACAGGAGT	-	9
37	CACCGAGGCTCCGCGCAGCGNNNN	chr1	18591731	hACaAGGaaTcTcTCCACAGGAGT	-	9
38	CACCGAGGCTCCGCGCAGCGNNNN	chr2	6479941	CtAgTcAGGaaTcTcTCCACAGGAGT	-	9
39	CACCGAGGCTCCGCGCAGCGNNNN	chr2	17447051	CtAgTcAGGaaTcTcTCCACAGGAGT	-	9
40	CACCGAGGCTCCGCGCAGCGNNNN	chr2	25423005	CtAgTcAGGaaTcTcTCCACAGGAGT	-	9
41	CACCGAGGCTCCGCGCAGCGNNNN	chr2	26959972	hACaAGGaaTcTcTCCACAGGAGT	-	9
42	CACCGAGGCTCCGCGCAGCGNNNN	chr2	28820020	hACaAGGaaTcTcTCCACAGGAGT	-	9
43	CACCGAGGCTCCGCGCAGCGNNNN	chr2	31672867	CtAgTcAGGaaTcTcTCCACAGGAGT	-	8
44	CACCGAGGCTCCGCGCAGCGNNNN	chr2	32697101	hACaAGGaaTcTcTCCACAGGAGT	-	8
45	CACCGAGGCTCCGCGCAGCGNNNN	chr2	32712871	hACaAGGaaTcTcTCCACAGGAGT	-	9
46	CACCGCCCAACTGAGTGAAGGTTNNNN	chr2	33490722	CtAgTcAGGaaTcTcTCCACAGGAGT	-	9
47	CACCGAGGCTCCGCGCAGCGNNNN	chr2	33501232	CACCGAGGaaTcTcTCCACAGGAGT	-	8
48	CACCGAGGCTCCGCGCAGCGNNNN	chr2	33951091	CtAgTcAGGaaTcTcTCCACAGGAGT	-	9
49	CACCGAGGCTCCGCGCAGCGNNNN	chr2	34517171	hACaAGGaaTcTcTCCACAGGAGT	-	9
50	CACCGAGGCTCCGCGCAGCGNNNN	chr2	47931225	CtAgTcAGGaaTcTcTCCACAGGAGT	-	9
51	CACCGAGGCTCCGCGCAGCGNNNN	chr2	49708239	CtAgTcAGGaaTcTcTCCACAGGAGT	-	9
52	CACCGAGGCTCCGCGCAGCGNNNN	chr2	57243714	hACaAGGaaTcTcTCCACAGGAGT	-	9
53	CACCGAGGCTCCGCGCAGCGNNNN	chr2	70241763	hACaAGGaaTcTcTCCACAGGAGT	-	9
54	CACCGCCCAACTGAGTGAAGGTTNNNN	chr2	73434964	gggCAAGGCTCTCCACAGGAGT	-	9
55	CACCGCCCAACTGAGTGAAGGTTNNNN	chr2	82053716	hCCCGCCCGTCTCCACAGGAGT	-	9
56	CACCGAGGCTCCGCGCAGCGNNNN	chr2	83958887	CtAgTcAGGaaTcTcTCCACAGGAGT	-	9
57	CACCGAGGCTCCGCGCAGCGNNNN	chr2	85791798	hACaAGGaaTcTcTCCACAGGAGT	-	9
58	CACCGAGGCTCCGCGCAGCGNNNN	chr2	93064802	CtAgTcAGGaaTcTcTCCACAGGAGT	-	9
59	CACCGAGGCTCCGCGCAGCGNNNN	chr2	93611661	gggCAAGGCTCTCCACAGGAGT	-	9
60	CACCGAGGCTCCGCGCAGCGNNNN	chr2	93645694	CtAgTcAGGaaTcTcTCCACAGGAGT	-	9
61	CACCGAGGCTCCGCGCAGCGNNNN	chr2	105069767	CtAgTcAGGaaTcTcTCCACAGGAGT	-	9
62	CACCGAGGCTCCGCGCAGCGNNNN	chr2	10517193	CtAgTcAGGaaTcTcTCCACAGGAGT	-	9
63	CACCGCCCAACTGAGTGAAGGTTNNNN	chr2	108600572	CtAgTcAGGaaTcTcTCCACAGGAGT	-	9
64	CACCGAGGCTCCGCGCAGCGNNNN	chr2	117143318	hACaAGGaaTcTcTCCACAGGAGT	-	8
65	CACCGAGGCTCCGCGCAGCGNNNN	chr2	119801515	hACaAGGaaTcTcTCCACAGGAGT	-	9
66	CACCGCCCAACTGAGTGAAGGTTNNNN	chr2	12681405	CtAgTcAGGaaTcTcTCCACAGGAGT	-	9
67	CACCGAGGCTCCGCGCAGCGNNNN	chr2	137089292	CtAgTcAGGaaTcTcTCCACAGGAGT	-	9
68	CACCGAGGCTCCGCGCAGCGNNNN	chr2	130267469	CtAgTcAGGaaTcTcTCCACAGGAGT	-	9
69	CACCGAGGCTCCGCGCAGCGNNNN	chr2	130564078	CtAgTcAGGaaTcTcTCCACAGGAGT	-	9
70	CACCGAGGCTCCGCGCAGCGNNNN	chr2	131064488	CtAgTcAGGaaTcTcTCCACAGGAGT	-	9
71	CACCGAGGCTCCGCGCAGCGNNNN	chr2	160732044	gggCAAGGCTCTCCACAGGAGT	-	9
72	CACCGAGGCTCCGCGCAGCGNNNN	chr2	160802250	CtAgTcAGGaaTcTcTCCACAGGAGT	-	7
73	CACCGAGGCTCCGCGCAGCGNNNN	chr2	162278882	CtAgTcAGGaaTcTcTCCACAGGAGT	-	9
74	CACCGAGGCTCCGCGCAGCGNNNN	chr2	16427644	CtAgTcAGGaaTcTcTCCACAGGAGT	-	9
75	CACCGCCCAACTGAGTGAAGGTTNNNN	chr2	164089776	hACaAGGaaTcTcTCCACAGGAGT	-	9
76	CACCGAGGCTCCGCGCAGCGNNNN	chr2	164688568	CtAgTcAGGaaTcTcTCCACAGGAGT	-	7
77	CACCGAGGCTCCGCGCAGCGNNNN	chr2	144852526	CtAgTcAGGaaTcTcTCCACAGGAGT	-	9
78	CACCGAGGCTCCGCGCAGCGNNNN	chr2	148043191	CtAgTcAGGaaTcTcTCCACAGGAGT	-	9
79	CACCGAGGCTCCGCGCAGCGNNNN	chr2	170015101	CtAgTcAGGaaTcTcTCCACAGGAGT	-	9
80	CACCGAGGCTCCGCGCAGCGNNNN	chr2	179914167	CtAgTcAGGaaTcTcTCCACAGGAGT	-	7
81	CACCGAGGCTCCGCGCAGCGNNNN	chr2	180212667	CtAgTcAGGaaTcTcTCCACAGGAGT	-	9
82	CACCGAGGCTCCGCGCAGCGNNNN	chr2	180514068	CtAgTcAGGaaTcTcTCCACAGGAGT	-	9
83	CACCGAGGCTCCGCGCAGCGNNNN	chr3	11083365	CtAgTcAGGaaTcTcTCCACAGGAGT	-	9
84	CACCGAGGCTCCGCGCAGCGNNNN	chr3	18621066	CtAgTcAGGaaTcTcTCCACAGGAGT	-	7
85	CACCGAGGCTCCGCGCAGCGNNNN	chr3	19951661	CtAgTcAGGaaTcTcTCCACAGGAGT	-	9
86	CACCGAGGCTCCGCGCAGCGNNNN	chr3	21671608	CtAgTcAGGaaTcTcTCCACAGGAGT	-	9
87	CACCGCCCAACTGAGTGAAGGTTNNNN	chr3	34729028	hACaAGGaaTcTcTCCACAGGAGT	-	8
88	CACCGAGGCTCCGCGCAGCGNNNN	chr3	38817310	CtAgTcAGGaaTcTcTCCACAGGAGT	-	8
89	CACCGCCCAACTGAGTGAAGGTTNNNN	chr3	48223820	CtAgTcAGGaaTcTcTCCACAGGAGT	-	9
90	CACCGAGGCTCCGCGCAGCGNNNN	chr3	51795844	CtAgTcAGGaaTcTcTCCACAGGAGT	-	9
91	CACCGAGGCTCCGCGCAGCGNNNN	chr3	52184474	CtAgTcAGGaaTcTcTCCACAGGAGT	-	9
92	CACCGAGGCTCCGCGCAGCGNNNN	chr3	55076356	CtAgTcAGGaaTcTcTCCACAGGAGT	-	9
93	CACCGAGGCTCCGCGCAGCGNNNN	chr3	57982282	CtAgTcAGGaaTcTcTCCACAGGAGT	-	8
94	CACCGAGGCTCCGCGCAGCGNNNN	chr3	60211772	hACaAGGaaTcTcTCCACAGGAGT	-	7
95	CACCGAGGCTCCGCGCAGCGNNNN	chr3	69544641	CtAgTcAGGaaTcTcTCCACAGGAGT	-	9
96	CACCGAGGCTCCGCGCAGCGNNNN	chr3	87805461	CtAgTcAGGaaTcTcTCCACAGGAGT	-	9
97	CACCGAGGCTCCGCGCAGCGNNNN	chr3	89390004	CtAgTcAGGaaTcTcTCCACAGGAGT	-	9
98	CACCGAGGCTCCGCGCAGCGNNNN	chr3	89911271	CtAgTcAGGaaTcTcTCCACAGGAGT	-	8
99	CACCGAGGCTCCGCGCAGCGNNNN	chr3	98329680	CtAgTcAGGaaTcTcTCCACAGGAGT	-	8
100	CACCGAGGCTCCGCGCAGCGNNNN	chr3	108428269	CtAgTcAGGaaTcTcTCCACAGGAGT	-	9
101	CACCGAGGCTCCGCGCAGCGNNNN	chr3	115997255	CtAgTcAGGaaTcTcTCCACAGGAGT	-	9
102	CACCGAGGCTCCGCGCAGCGNNNN	chr3	116888807	CtAgTcAGGaaTcTcTCCACAGGAGT	-	9
103	CACCGAGGCTCCGCGCAGCGNNNN	chr3	11763745	CtAgTcAGGaaTcTcTCCACAGGAGT	-	9
104	CACCGAGGCTCCGCGCAGCGNNNN	chr3	119121716	CtAgTcAGGaaTcTcTCCACAGGAGT	-	9
105	CACCGCCCAACTGAGTGAAGGTTNNNN	chr3	12783845	CtAgTcAGGaaTcTcTCCACAGGAGT	-	9
106	CACCGAGGCTCCGCGCAGCGNNNN	chr3	130060135	CtAgTcAGGaaTcTcTCCACAGGAGT	-	9
107	CACCGAGGCTCCGCGCAGCGNNNN	chr3	13031978	CtAgTcAGGaaTcTcTCCACAGGAGT	-	9
108	CACCGAGGCTCCGCGCAGCGNNNN	chr3	131116757	gggCAAGGCTCTCCACAGGAGT	-	9
109	CACCGAGGCTCCGCGCAGCGNNNN	chr3	131471628	CtAgTcAGGaaTcTcTCCACAGGAGT	-	8
110	CACCGAGGCTCCGCGCAGCGNNNN	chr3	147117148	CtAgTcAGGaaTcTcTCCACAGGAGT	-	9
111	CACCGAGGCTCCGCGCAGCGNNNN	chr3	15327915	CtAgTcAGGaaTcTcTCCACAGGAGT	-	9
112	CACCGAGGCTCCGCGCAGCGNNNN	chr3	153488448	CtAgTcAGGaaTcTcTCCACAGGAGT	-	9
113	CACCGAGGCTCCGCGCAGCGNNNN	chr3	154251972	hACaAGGaaTcTcTCCACAGGAGT	-	9
114	CACCGAGGCTCCGCGCAGCGNNNN	chr4	8579745	CtAgTcAGGaaTcTcTCCACAGGAGT	-	9
115	CACCGAGGCTCCGCGCAGCGNNNN	chr4	18029183	CtAgTcAGGaaTcTcTCCACAGGAGT	-	9
116	CACCGAGGCTCCGCGCAGCGNNNN	chr4	24631445	CtAgTcAGGaaTcTcTCCACAGGAGT	-	9
117	CACCGCCCAACTGAGTGAAGGTTNNNN	chr4	31636941	CtAgTcAGGaaTcTcTCCACAGGAGT	-	9
118	CACCGAGGCTCCGCGCAGCGNNNN	chr4	3371468	CtAgTcAGGaaTcTcTCCACAGGAGT	-	9
119	CACCGAGGCTCCGCGCAGCGNNNN	chr4	37001740	CtAgTcAGGaaTcTcTCCACAGGAGT	-	7
120	CACCGAGGCTCCGCGCAGCGNNNN	chr4	37063381	CtAgTcAGGaaTcTcTCCACAGGAGT	-	9
121	CACCGAGGCTCCGCGCAGCGNNNN	chr4	38565722	hACaAGGaaTcTcTCCACAGGAGT	-	9
122	CACCGAGGCTCCGCGCAGCGNNNN	chr4	41611043	CtAgTcAGGaaTcTcTCCACAGGAGT	-	8
123	CACCGAGGCTCCGCGCAGCGNNNN	chr4	43616317	CtAgTcAGGaaTcTcTCCACAGGAGT	-	9
124	CACCGAGGCTCCGCGCAGCGNNNN	chr4	43612620	CtAgTcAGGaaTcTcTCCACAGGAGT	-	9
125	CACCGAGGCTCCGCGCAGCGNNNN	chr4	46610409	CtAgTcAGGaaTcTcTCCACAGGAGT	-	9
126	CACCGAGGCTCCGCGCAGCGNNNN	chr4	48027887	hACaAGGaaTcTcTCCACAGGAGT	-	9
127	CACCGAGGCTCCGCGCAGCGNNNN	chr4	49151262	CtAgTcAGGaaTcTcTCCACAGGAGT	-	9
128	CACCGCCCAACTGAGTGAAGGTTNNNN	chr4	5345042	hACaAGGaaTcTcTCCACAGGAGT	-	9
129	CACCGAGGCTCCGCGCAGCGNNNN	chr4	56611614	CtAgTcAGGaaTcTcTCCACAGGAGT	-	9
130	CACCGAGGCTCCGCGCAGCGNNNN	chr4	57847249	CtAgTcAGGaaTcTcTCCACAGGAGT	-	8
131	CACCGAGGCTCCGCGCAGCGNNNN	chr4	63212225	CtAgTcAGGaaTcTcTCCACAGGAGT	-	9
132	CACCGAGGCTCCGCGCAGCGNNNN	chr4	63297973	hACaAGGaaTcTcTCCACAGGAGT	-	9
133	CACCGAGGCTCCGCGCAGCGNNNN	chr4	103500698	hACaAGGaaTcTcTCCACAGGAGT	-	9
134	CACCGAGGCTCCGCGCAGCGNNNN	chr4	10748668	CtAgTcAGGaaTcTcTCCACAGGAGT	-	9
135	CACCGAGGCTCCGCGCAGCGNNNN	chr4	10805241	hACaAGGaaTcTcTCCACAGGAGT	-	9
136	CACCGAGGCTCCGCGCAGCGNNNN	chr4	109800272	CtAgTcAGGaaTcTcTCCACAGGAGT	-	9
137	CACCGCCCAACTGAGTGAAGGTTNNNN	chr4	114586084	CtAgTcAGGaaTcTcTCCACAGGAGT	-	9
138	CACCGAGGCTCCGCGCAGCGNNNN	chr4	114597689	CtAgTcAGGaaTcTcTCCACAGGAGT	-	9
139	CACCGAGGCTCCGCGCAGCGNNNN	chr4	118003031	gggCAAGGCTCTCCACAGGAGT	-	9
140	CACCGAGGCTCCGCGCAGCGNNNN	chr4	119990866	hACaAGGaaTcTcTCCACAGGAGT	-	9
141	CACCGCCCAACTGAGTGAAGGTTNNNN	chr4	12074899	hACaAGGaaTcTcTCCACAGGAGT	-	9
142	CACCGAGGCTCCGCGCAGCGNNNN	chr4	123704443	CtAgTcAGGaaTcTcTCCACAGGAGT	-	9
143	CACCGAGGCTCCGCGCAGCGNNNN	chr4	12458674	CtAgTcAGGaaTcTcTCCACAGGAGT	-	7
144	CACCGAGGCTCCGCGCAGCGNNNN	chr4	12501786	CtAgTcAGGaaTcTcTCCACAGGAGT</		

Supplemental Table 6. Primers, plasmids and sgRNAs used in this study

	Name	Sequences (5' to 3')	ID Number
Primers	U6_gRNA_PCR_F	GAG GGC CTA TTT CCC ATG ATT CCT	RDC 255
	dTomato_guide_B	AAA CCA CTG TGG GGT GGA GGG GAC	RDC 1194
	mGAPDH F	TGTTTGTGATGGGTGTGAACC	RDC 345
	mGAPDH R	ACTGTGGTCATGAGCCCTTC	RDC 346
	Lama1 Primer FW	GGAAGGTTACAAAGTTCGATTGG	RDC 977
	Lama1 Primer RV	ACGTGAAATAAGACCTTGCCATC	RDC 978
	Lama1 qPCR 1 KL F	TTTCTTTGAAGGAAGCGGATATG	RDC 1918
	Lama1 qPCR 2 KL F	TGGGTCCATTAACAGAAGGAAAG	RDC 1919
	Lama1 qPCR 2 KL R	ATGGGTGAAGTCCAAAAGTTGAG	RDC 1920
	Vector genome F	ATGGTGAGCAAGGGCGAGG	RDC 1687
	Vector genome R	AGCTTGCCGTAGGTGGCATC	RDC 1679

	Name	ID number
Plasmids	minCMV-tdTomato	RDC 262
	px601 SadCas9-VP64	RDC 153
	3-guide cassettes	RDC 367

	Name	Sequences (5' to 3')	PAM
sgRNAs	<i>tdTomato</i> sgRNA Top	CACCGTCCCCTCCACCCACAGTG	AAGAAT
	<i>tdTomato</i> sgRNA Bottom	AAACCACTGTGGGGTGGAGGGGAC	
	<i>Lama1</i> sgRNA1 Top	CACCGAAGGGCCTGCGCACCAGGC	CAGGGT
	<i>Lama1</i> sgRNA1 Bottom	AAACGCCTGGTGCAGGCCCTTC	
	<i>Lama1</i> sgRNA2 Top	CACCGCGGGGCGCGCCAGGCAGGC	GGGGGT
	<i>Lama1</i> sgRNA2 Bottom	AAACGCCTGCCTGGCCGCGCCCGC	
	<i>Lama1</i> sgRNA3 Top	CACCGTCCAGGGGGAGCCCCGCCGTG	CGGAGT
	<i>Lama1</i> sgRNA3 Bottom	AAACCACGGCGGGGCTCCCCCTGGAC	
	<i>Lama1</i> sgRNA4 Top	CACCGGTGGTGGCGGGGTGCCTCTC	CTGGGT
	<i>Lama1</i> sgRNA4 Bottom	AAACGAGAGGCACCCCGCCACCACC	
<i>Lama1</i> sgRNA5 Top	CACCGACCCCACTGGAGTGGAGGGT	CAGAGT	
<i>Lama1</i> sgRNA5 Bottom	AAACACCCTCCACTCCAGTTGGGGTC		